Mapana Journal of Sciences
2020, Vol. 19, No. 1, 87-137
ISSN 0975-3303|https://doi.org/10.12723/mjs.52.5

Graphene-based Materials for Supercapacitors

Imran Jafri*, Anish Thomas†, Meera Varghese‡,
Sanjay Acharya§, Joseph Sebi** Akshaya Sasindran Nair#

Abstract

The adoption of more environmental-friendly means of harnessing and storing energy while minimising harmful effects on the environment is becoming more significant. Supercapacitors are becoming a more favoured means of energy storage systems owing to their higher surface area electrodes and thinner dielectrics. For greater capacitances, a suitable material must have high porosity. Such a suitable material is carbon, most notably graphene, with superior electrical properties, chemical stability and high surface area. This review focuses on the types of mechanism for storing energy, the types of materials used in supercapacitors and the applications and scope of supercapacitor research and development.

Keywords: Supercapacitors, Electrode, Energy Storage, Graphene, Activated Carbon

1. Introduction

Increasing demand for energy consumption has caused more and more natural resources to deplete. As vital as it is to adopt more

*Department of Physics and Electronics(DPE), CHRIST (Deemed to be University)(CU), Bengaluru, India; imran.jafri@christuniversity.in
† (DPE)(CU), Bengaluru, India; anishthomas9555@gmail.com
‡ (DPE)(CU),, Bengaluru, India; meeravarghese04@gmail.com
§ (DPE)(CU), Bengaluru, India; sanjaykota100@gmail.com
** (DPE)(CU), Bengaluru, India; josephsebic3@gmail.com
#(DPE)(CU), Bengaluru, India;akshayas858@gmail.com

eco-friendly means of obtaining energy, it is equally important to use the energy in a safe and non-hazardous manner. Thus, substantial research is being undertaken to design and manufacture methods and materials that are more efficient. Supercapacitors (SC) are such devices with attracting advantages that could surpass that of conventional batteries in an increasing number of applications in energy storage [1, 2].

Supercapacitors, also known as ultracapacitors, differ from conventional capacitors, in which they utilise higher surface area electrodes to achieve capacitances and thus high energy densities greater than that of fuel cells whilst maintaining the high-power output of standard capacitors. In a way, they are similar to batteries in terms of energy storage capacity but deliver a higher power output, which is sometimes necessary. In modern applications, supercapacitors bring a wide range of advantages such as minimal space occupation, operation in extreme conditions, improved load balancing when used in parallel with a battery, and extended battery run time and battery life. They can be seen in general applications such as in consumer electronics to stabilise power supply, in energy harvesting applications that involve storing energy from renewable sources in storage devices, transport applications such as emergency actuators for doors in aeroplanes, or in hybrid vehicles to provide acceleration via bursts of power. They can also be used in parallel with batteries to provide a short high burst of power in certain machines that require a kick-start, and that can later be recharged [3]. In general, they can be classified into application classes such as memory backup, energy storage, power, and instantaneous power, based on their discharge levels [4].

In an SC, there are no chemical reactions involved in the energy storage mechanism. This makes the supercapacitor an electrostatic device storing the energy as an electric field between the two conducting electrodes. Hence, a large part of an SC's functionality lies in the nature and efficiency of the material used as the electrode, as the SC mainly relies on the electrode surface area. There are many factors to take into notice when considering the feasibility of a material, such as an abundance, porosity and the cost of manufacturing. Good conductivity, high inertness, high

corrosion resistance, and environmental friendliness must be brought to concern as well. Thus, a suitable material is carbon, in various forms such as activated carbon, graphite, graphene, carbon-fibre cloth and carbon nanotubes [5].

Of these allotropes, graphene, a single-atom-thick sheet of carbon atoms, arranged in a regular hexagonal pattern, is a highly effective prospective material. With advantages of high thermal conductivity, electrical conductivity, strength, and exceptional surface area of up to 2675 m^2/g, its two-dimensional structure allows for greater charge and discharge functions, where charge carriers can easily enter and exit the electrodes without much difficulty. This allows for the graphene to be utilised in filter applications which cannot apply to other carbon materials [6].

This paper gives an overview of the types of the mechanism of how different SCs work, following which the graphene material will be explored as a suitable material for electrodes in SCs, bringing notice to its different types and characteristics, as well as its limitations. There are numerous applications for SCs in the present. Future possibilities for SCs are also discussed keeping in mind the current trends and developments in SC materials.

2. Energy Storage Mechanism in Supercapacitors

Supercapacitors have drawn significant attention with promising energy storage devices boasting of high power density, exceptional cycle stability, and stable operation over a wide range of temperature and low internal resistance. The lithium-ion batteries that now power almost all consumer electronics devices store a great deal of energy but are limited with extended downtimes of operation and poor cycle life. On the other hand, capacitors can charge and discharge quickly. SC provides the best of both options and acts as the bridge between capacitors and batteries. In SC, the reversible reaction on the surface of electrodes (charge separation and faradic redox reaction at the electrode/electrolyte interface) serves as the major energy storage of the system. Since the specific surface bulk ionic diffusion does not take part within the interior crystalline regions the SC is capable of delivering a high power density (i.e., charge/discharge at an ultrafast rate). Conversely, the

relatively low energy density (poor specific capacitance) and high cost are the two major challenges which complicate the efforts to replace batteries by SCs. To overcome these shortcomings, the electrode materials have been a point of interest in recent years. The emergence of Graphene has drastically improved the performance of SC [7].

The energy storage mechanism in SCs is of several types namely electric, double-layer, capacitor, (EDLC) and, pseudocapacitor (PC). The EDLC stores charge electrostatically at the interface of its electrode and electrolyte whereas pseudocapacitive materials make use of the exchanging of faradic charges [8, 9].

2.1 Electrochemical Double Layer Capacitor

An EDLC comprises two conducting electrodes insulated by a porous separator immersed in an electrolyte. While applying the current, potential difference develops between two electrodes and the anions and cations are physically absorbed on the respective surfaces of electrodes. This reversible reaction highly depends upon the electrical field strength across the electrode and electrolyte and the chemical affinities between them. The schematic demonstration of the EDLC mechanism in an SC with porous carbon conducting materials is shown below in Fig.1.

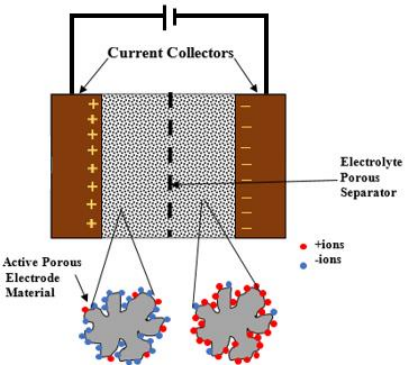

Figure.1: Schematic for an EDLC with Porous Electrodes.

Several models were suggested to explain the performance of EDLC. Among them, the Helmholtz model, which is the first and simplest model, assumes the EDL phenomenon as the adsorption and neutralisation of opposite sign ions at the electrode-electrolyte interface. The layered opposite charges are separated by an atomic distance that creates a conventional capacitor structure [2]. The model assumes an infinite rate of ion diffusion. Bringing modifications to this model Gouy and Chapman suggested a diffusive layer model (Gouy-Chapman Model) which provided a more sophisticated picture of the EDL. According to this model, a diffused double layer of oppositely charged ions concentrates in a liquid surrounding a charged surface. The concentration of the ions follows the Boltzmann distribution. The Gouy-Chapman Model assumes the ions as point charges that can freely approach the electrode surface [10]. This model does not hold good for highly charged double layers. The Gouy-Chapman-Stern model combines the Helmholtz model and the Gouy-Chapman Model assuming that in addition to the diffusive layer (Gouy-Chapman layer) as suggested by Helmholtz there could be an inner region called Stern layer (Helmholtz layer). The Stern layer forms by the adherence of some surface-adsorbed ions to the electrode [11]. The ions are assumed to have a finite size so that they may be able to get the closest approach to the electrode approximately of the ionic radius. No free charges exist in the stern layer whereas mobile ions are present in the diffusive layer [12]. The total EDL capacitance can be treated as the combination of Stern Layer Capacitance and diffusive layer capacitance. In mathematical terms, it can be represented as,

$$\frac{1}{Cdiff} = \frac{1}{Cs} + \frac{1}{CDL} \tag{1}$$

where C_{diff} is the total EDL Capacitance, Cs is the Stern Layer Capacitance and C_{DL} is the Diffusive Layer Capacitance [13]. The schematic representation of the various models for EDL is shown in Fig.2.

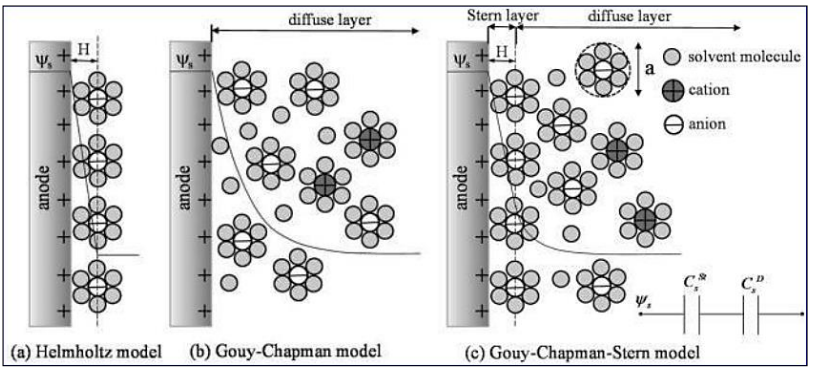

Figure 2: Schematics of models for the electric double layer at a positively charged surface: (a) Helmholtz model, (b) Gouy-Chapman model, and (c) Gouy-Chapman-Stern model. [Reprinted with permission from Ref. CITATION Hai11 \l 1033 [12] Copyright (2011) American Chemical Society.]

None of the aforementioned models could satisfactorily explain the actual performance of porous SC electrodes. The impact of different pore shapes on capacitance performance is still unknown [11].

As mentioned above in EDLC, the double layer of charges at the electrode surface separated by a molecular distance can act as a physical capacitor. The charge formation and relaxation are nearly instantaneous with a time constant ~10^{-8}s. As this mechanism does not involve chemical reactions but a charge rearrangement, the EDLC exhibits a rapid response to potential changes. From Figure.2., the specific capacitance and available surface area are closely related to one another. The affinity of the mass transference route, constraints of the area of the pores and the wettability of the pore surface governs the transportation of the particles [14]. For an EDLC, the specific capacitance is given by,

$$C = \varepsilon_0 \cdot \varepsilon_r \cdot \frac{A}{d} \tag{2}$$

where ε_0 is the vacuum permittivity (ε_0 = 8.854 × 10^{-12} F/ m), ε_r is the dielectric constant of the electrolyte, A is the available specific surface area of the electrode and d is the Debye length (effective thickness of the double layer). Fig.3. depicts the charging and discharging process of an EDLC [2].

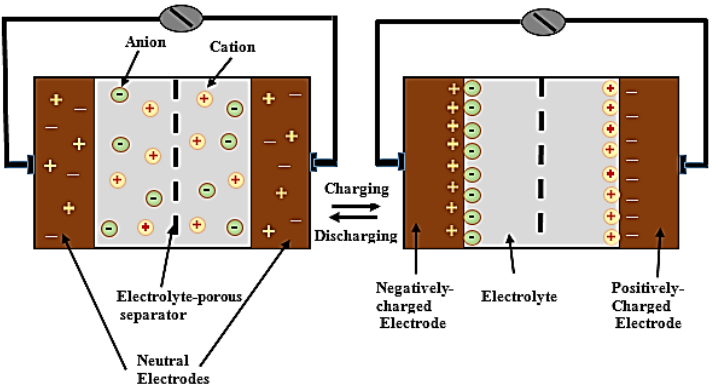

Figure 3: Schematic Illustration of Charging Process in EDLC

EDLC offers higher energy density than conventional capacitors because of their large surface area with a porous structure and the small charge separation distances. However, the electrostatic surface charging mechanism involving in EDLC limits energy density to a relatively lower value than that of the batteries. The stress and swelling on the active material are avoided by the absence of faradic reactions and provides high stability to the device [15, 16, 2].

2.2 Pseudo-Capacitors

In a pseudocapacitor, the energy storage mechanism is a hybrid between a battery and an EDLC, which involves the surface electrosorption and Chemical process. Since the charge storage is in the bulk of the material due to high-redox reaction that behaves as capacitance and in which the electrons are transferred between electrodes and the electrolyte, it is known as Pseudo-Capacitors. The charge transfer occurs at a fast rate due to the lower penetration of the ions from the electrolyte. These reactions, which affect EDLC, results in considerable progress in the capacitive performance of the device. The charge storage mechanism in a pseudocapacitor is schematically given in Fig.4.

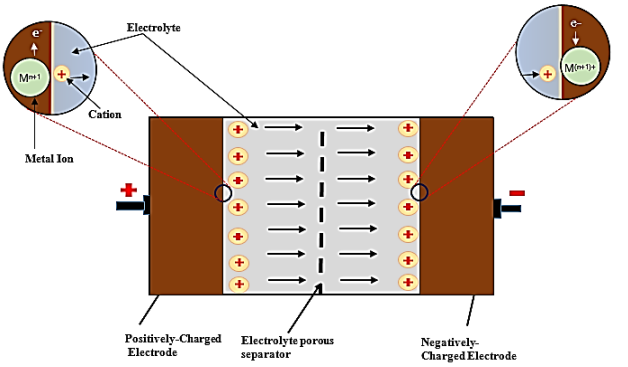

Figure 4: Schematic for the Mechanism of a Basic Pseudocapacitor.

The differences associated with the physical processes and with the types of materials results in the occurrence of three different faradaic mechanisms that contribute towards the pseudocapacitance, which are the under-potential deposition, redox pseudocapacitance, and the intercalation pseudocapacitance [17, 18, 19].

In the under-potential deposition, in the presence of an applied potential, an adsorption layer of metal ions forms on the electrode surface made of another kind of metal. The electrosorption of Pb on Au is a typical example of the aforementioned mechanism. In redox pseudocapacitance, the mechanism involves the electrochemical adsorption of electroactive ions onto the electrode surface or to its surroundings. The redox reactions involve the changes in the oxidational state of the elements involved in the reaction. It may be the lowering of the oxidation state by the acceptance of the electrons or the raising of the oxidation state because of the releasing of electrons. The redox pseudocapacitance displayed by the ruthenium oxide is an example. The intercalation pseudocapacitance involves the insertion of ions into the solid electrode lattice. In the intercalation process, the electrical neutrality of the electrode is preserved and no crystallographic phase change occurs with the faradaic charge-transfer. The presence of an appropriate reducing agent, the existence of unpopulated states, the occurrence of easily accessible bands beyond the Fermi level and the maintenance of the orientation of elements in the lattice during the insertion process are the

conditions to be satisfied for the intercalation mechanism. The intercalation of Li^+ into TiS_2 is an example. Fig.5. shows schematic of three different faradaic mechanisms associated with the pseudocapacitance.

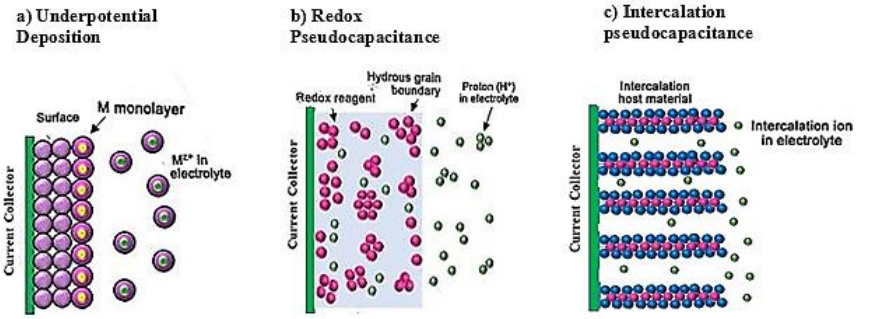

Figure 5: Schematic of different Faradaic Processes that give rise to Pseudocapacitance.

The occurrence of multiple charge storage mechanisms raises the capacitance to higher values but, the power performance of the pseudocapacitor lowers by the slower faradaic process. Moreover, the electrode materials that swell and contract with the charging and discharging cycles show a reduced lifespan.

Neither EDLC nor pseudocapacitance alone can satisfy the energy and power density requirements appreciably; hence, a better way to attain an improved energy density without altering the power density is the combination of EDLC and pseudocapacitor, i.e. the Hybrid SCs [20, 21].

3. Activated Carbon

Presently, many carbonaceous materials are used such as waste, coal, nutshells and wood to exhibit larger surface area, good electrical performance and affordable cost by a physical and chemical process. Thermal treatment of carbon precursor undergoes physical activation at a high temperature of around 700°c - 1200° using an oxidising agent and a reducing agent. Lower temperature involves chemical treatment around 400°c to 700°c by chemical agents like oxyacid, potash, metal chloride or hydroxide knowing activation method and the materials used. The micro,

meso, and macroporous structure of activated carbon is created through the activated process to enhance the surface area of activated carbon up to 3000 m^2/g and to improve their electrochemical property. Available surface area, pore size distribution, structure and shape, surface functionality and conductivity all have a larger influence in the performance of EDLCs.

3.1. Porous Carbon Material

Ba et al [2] have developed SCs electrodes using chemical activation of fig waste which gave high porosity, well-organised micro, meso, and macropores with a specific capacitance of 340 to 217 F/g at current density 0.5 and 20 A/g with 99% of capacitance retention after 10,000 cycles. This result makes clear that electrical performance of activated carbon dominates than carbon-based Nanostructure, graphene and CNT Including activated carbon from waste such as sugarcane, bagasse, corn grains, cellulose. Excessive activation leads to higher pore volumes, which reduces material density, conductivity, and lower power capability. Therefore, higher specific area of activated carbon increases the specific surface area. Knowing that organic electrolytes with acidic functionalities and moisture content are contributed by activated carbon, to correlate between capacitance performance and nano-porous structure using different electrolytes and higher specific capacitance is aimed for. Capacitance in aqueous electrolytes (100-300F/g) is higher than organic electrolytes (less than 150 F/g) since in organic electrolytes, ions are larger than those in water-based electrolytes. These organic electrolytes increase the quality of pores that are smaller than the ions which increase the number of pores that do not take part in the charge storage mechanism.

Using pre-cross-linked lignin gel, mesoporous carbon is synthesised with pore formation agents and activating the carbon through a chemical and physical process. 1.5-to 6-fold increase in porosity with maximum Brunauer-Emmett-Teller (BET) specific area of 1148 m2/g is obtained. Biomass-derived mesoporous carbon materials show potential for specific electrochemical applications use.

Mesoporous carbons involve carbonising carbon precursor and removal of the scaffold. Next to cellulose and chitin, lignin is the most abundant natural polymer, with low cost and synthesis of suitable mesoporous carbon.

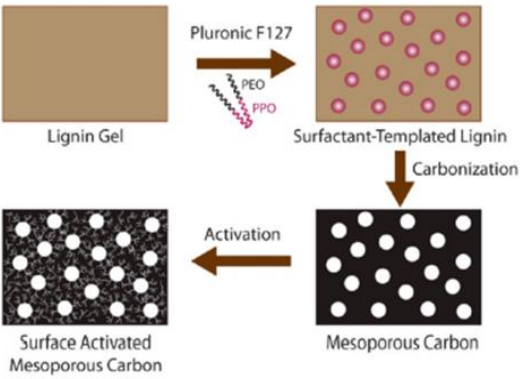

Figure 6: Represents Activation Carbon Synthesis from a lignin precursor getting a surfactant templated mesoporous carbon. [Reprinted with permission from Ref. [22] Copyright (2014) American Chemical Society.]

3.2. Activation of Activated Carbon

Surface activation of mesoporous carbon with carbon dioxide and potassium hydroxide is done to increase its porosity at high temperature and is continued with characterisation technique like TEM and X-ray photoelectron spectroscopy. The synthesis of mesoporous carbon from lignin is undergone, followed by activation of mesoporous carbon, characterisation of precursor carbons and then electrochemical measurement. Increase in pristine mesoporous volume is noted by using carbon dioxide and potassium hydroxide with physical and chemical activation method around 875-1000 degree Celsius. After analysis with x-ray photoelectron and electron microscope, there is less amount of graphitic structure in all carbon materials and the presence of the oxygen-containing functional group in all carbons [22].

After the synthesis of mesoporous carbons as SCs electrodes materials, with gravimetric specific capacitances of 77.1, 102.3 and 91.7 F/g for original ones, carbon dioxide activated with 56% burn off and potassium hydroxide activated 200% loading carbons. After the activation of original carbon, capacitances of 102.3 and 91.7 F/g

is obtained. The reduction of carbon footprint and boosting the economy of lignin producing mill enhancement of sustainability of lignin-based carbon materials is seen with controlled porosity [22].

With high temperature, carbonisation and activation with potassium hydroxide to prepare activated carbon, an amorphous character is shown in resulting activated carbon materials and its porous structure with high specific area ranging from 2245 m^2g^{-1} to 2841 m^2g^{-1}. In the presence of potassium hydroxide electrolyte, activated carbons exhibit ideal capacitive behaviour with a maximum specific capacitance of 330 F g^{-1}, at a current density of $1Ag^{-1}$. After 2000 cycles 92% of initial capacitance being retained, new biomass source is obtained with high-performance SCs and low-cost energy storage devices.

Various biomass materials like dates, stones, coconut shells, pitch coke, wood, rice husk, walnut shell, banana peel and fungi have been used as precursors to produce activated carbon and have been implemented as electrode materials, adsorbent and catalyst carriers.

To get the activated carbon concentrating on waste, tea leaves are a huge natural resource having a chemical composition of around 3.5-7.0% and inorganic substance composition of 93.0- 96.5%.

Moderate cost, good chemical stability and high electrical conductivity and activated carbon content with porous structure and high specific area make them a suitable choice.

When the water temperature reaches room temperature, the tea leaves are soaked with boiling water then pyrolysis of dried tea leaves is carried out at 600 degree Celsius for 2 hours in the horizontal tube with argon flow of 40 scum under argon atmosphere and potassium hydroxide activation to obtain carbon products. Considering various types of carbon materials, KOH activation is adopted to increase the surface area and improve electrochemical performance. As the activation temperature reaches more than 700 degree Celsius, decomposition of potassium carbonate takes place along with carbon. Weight loss and yields of five types X-ACs are around 0.5 through the activation of carbonate X-Cs KOH at 800 degree Celsius for 1-hour leading to nanoscale pores of large amounts [23].

3.3. Mesopores and Micropores

Using petroleum-based precursors as activated carbon for electrode materials in SCs poses an increase in demand for energy supply and environmental sustainability, thus utilising waste tires as to produce activated carbon materials by chemical activation and pyrolysis method. Activated carbons are tailored to obtain multiple physical properties. Since specific capacitance depends on statistical means, multiple regression and stepwise regression methods are employed here for porosity and activated carbon electrodes. Carbon electrodes are controlled by micropore volume but are not dependent on mesopore volume. Mesopore and micropore volume increases the capacity rate instead of the absolute value of mesopore volume.

Matching mesopore volume must match with micropore volume to get maximum rate capability for EDLC-based electrodes, thus relying on four main factors:

I. Diffusion of ions in liquid electrolyte

II. Charge transfer at the electrolyte and electrode interface.

III. Ions absorbers on the surface of a solid electrode

IV. Electron transport in a solid electrode and the whole circuit [24].

By one-step pyrolysis techniques using biomass sago bark, carbon nanosphere is synthesised. The porous nature and available 95% amount of carbon amount is synthesised with particle size ranging between 40-70 nm. The Specific Capacitance of 180F/g at 2mV/s and cyclic stability up to 1700 cycles, makes it useful in SC applications. Sago bark has its cellulosic – hemicellulose and lignin content to produce Carbon nanospheres. It is treated as a raw material by pyrolysis technique with ultra-small-sized nanosphere of carbon. Carbon nanospheres are obtained from sago waste ranging from size 40-70nm with bulk production. Application of SCs is relayed due to its specific capacitance, which is less toxic [25].

Volumetric energy density and loss of power capability is seen with a larger amount of activation, which leads to a high pore volume which results in low conductivity and low material density.

Organic electrolytes having a pore size smaller than those of ions do increases the charge storage, wettability of carbon surface, determined by chemical affinity. The surface functionalities play a major role in carbon electrode performance, where it increases the electrolyte ions in carbon materials, oxygen functional group with low porosity in high concentrations [26].

Using orange peel through chemical activation method by Hydrogen Peroxide and its electrocatalyst, the material undergoes various structural, compositional and electrochemical studies. Platinum loaded onto activated carbon is investigated by cyclic voltammetry (CV) in Nitrogen and Oxygen saturated in aqueous $HClO_4$. Using CV, the electrochemical surface area of activated carbon from orange peel is examined. Scanning Electron Microscope (SEM) and X-ray Diffraction (XRD) technique enable to relate the physical properties of activated carbon. Orange peel is derived to get activated carbon with a high specific area around 275 F/g at 10mv/s scan rate. Orange peel is made to treat with orthophosphoric acid by pyrolysis method at 600-degree Celsius by simple activation method. Carbon content which is highly amorphous and FTIR analysis confirms the stretching vibrations of C-C, C-O, O-H. CV data of OP-Activated carbon electrode indicates specific capacitance to perform Oxygen reduction agent [27].

Adsorption of both gases and solutes from aqueous solution using high porosity activated carbon material gives the separation of gases and recovery of solvents and removal of organic pollutants from drinking water and a catalyst. By two-activation procedure, activation of reedy grass leaves with KOH covers the operation parameters as time and temperature activation and impregnation ratio for product quality. BET method and iodine number method characterisation technique signify the product quality [28].

Activation carbon by wood char or coal char or simply partially de-volatilised carbon materials dominates as an adsorbent. Considering environmental benefits, lignocellulose material and biomass sources are used to produce activated carbon, which gives the final microstructure and material characteristics with properties of carbon materials thereby giving the applications in adsorption of heavy metals, dyes, volatile organic compounds, gas storage and electrochemical capacitors [29].

3.4 Advantages of Graphene Material as Electrode than Activated Carbon

Natural mineral obtained contains graphene material, which in the past 500 years is widely used in daily life like pencils and dry lubricants; it possesses lower electrical resistance and good electrode materials for SCs application with high thermal conductivity. Considering graphene as an electrode material, it gives stretchable property which with chemically modified graphene sheets helps to tune with different types of electrolyte ion since they are independent of binders and conductive fillers [30].

Graphene has a substantially higher surface area compared to activated carbon, better electrostatic charge storage for SC applications. Graphene with single atomic layer is lighter than activated carbon with the best way of energy storage. Graphene with elastic property and mechanical strength coupled with minimal cost and light weightiness makes it a good electrode for SCs. Energy storage in Graphene materials has high charge and discharge rates [31].

For graphene, high conductivity and high surface area by the combination of two carbon nanomaterials such as nanotube delivers the most advantage. The carbon nanotubes connect the uniform network capacitance of activated carbon having the capacitance of 250F/g [32].

4. Graphene-Based Supercapacitor Electrodes

The viability of SCs considerably depends on the anode and cathode materials. The expected properties of these electrodes are high surface area per unit weight, good electrical conductivity and high capacitance. They should be physically robust also so that, they do not degrade during the operation. The carbon materials found to be the best to meet these requirements for SC applications. Among the various carbon materials, graphene has received immense attention of the researchers [16]. Graphene is a two-dimensional monolayer of Graphite, having outstanding physical, mechanical and chemical properties and hence can act as high-performance SC electrodes. The advantage of graphene-based SCs are; they exhibit extremely high electrical and thermal conductivity,

highly tunable surface area, strong mechanical and electrical stability and they are light in weight. Conversely, the application of pure graphene as SC electrodes is restricted by the poor efficiency due to agglomeration, which is the restacking of graphene sheets through Van der Waal forces to form Graphite and results in the reduction of surface area. To fix this problem and ensure satisfactory specific capacitance methods like heteroatom doping, the formation of three-dimensional frameworks and so on are followed. It is also helpful to achieve long and continuous transferring of electrons and maintain short ionic diffusion distances. The various graphene structures such as zero-dimensional graphene dots or powders, one-dimensional graphene fibres and yarns, two-dimensional films and sheets of graphene, three-dimensional structures like graphene composites, graphene foams and so on can be served as supercapacitor electrodes [33, 9].

CV and Galvanostatic charge-discharge (GCD) are two extensive techniques to analyse the electrochemical behaviour of SC. CV is useful to study the oxidation-reduction reactions involved in the charge storage mechanism of SC. It records the flow of current through the electrochemical cell concerning the variations in the applied potential. It is an effective method to estimate the capacitance value of the electrode. In contrast, GCD tests operate under a constant charge/discharge current density within an applied voltage window range. It is a useful method in determining cycling stability, capacitance and energy and power densities of SC [11, 2]. The CV and GCD performance results of a graphene-based SC synthesised by Khakpour et al. [34] through bipolar exfoliation and in situ deposition methods is given in Fig.7.

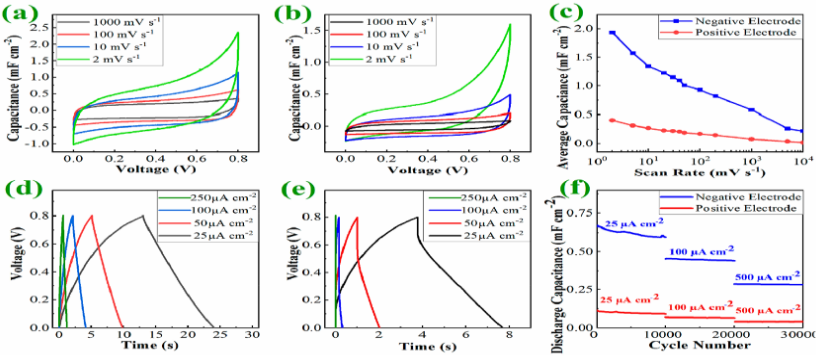

Figure 7: Cyclic voltammograms for (a) negative electrode and (b) positive electrode based typical supercapacitor at different scan rates; (c) Average areal capacitance at positive and negative electrode at different scan rates; (d), (e) Galvanic charge –discharge curve; (f) Cycling stability performance for a typical graphene electrode. [Reprinted with permission from Ref.CITATION Ima19 \l 1033 [34] Copyright (2019) American Chemical Society.]

A good number of SC research presently being conducted concentrates on graphene-based materials. However, it is not easy to synthesise pristine graphene on an industrial scale in a profitable way. Moreover, due to the layer stacking (agglomeration) effect, practically it is unable to attain the theoretical surface area (~ 2600 m^2/g) and the maximum specific capacitance (~ 550 F/g) of graphene. Hence, various attempts have been devoted to overcoming these challenges and to a great extent, the usage of different structures of graphene found to be an effective solution for the aforementioned issues [15]. Some of the research efforts held in this area are discussed below.

4.1. Pure Graphene electrodes

Graphene dots can be obtained by the controllable reduction of graphene oxide (GO) which is derived through the chemical exfoliation of Graphite. Usually, a reducing agent such as hydrazine hydrate is used. The resultant material with high surface area and good electrical conductivity offer a fast rate of charge transferring and high power density but the agglomeration tendency limits the further processing in an aqueous environment as the reduced graphene oxide (rGO) become hydrophobic [20, 8].

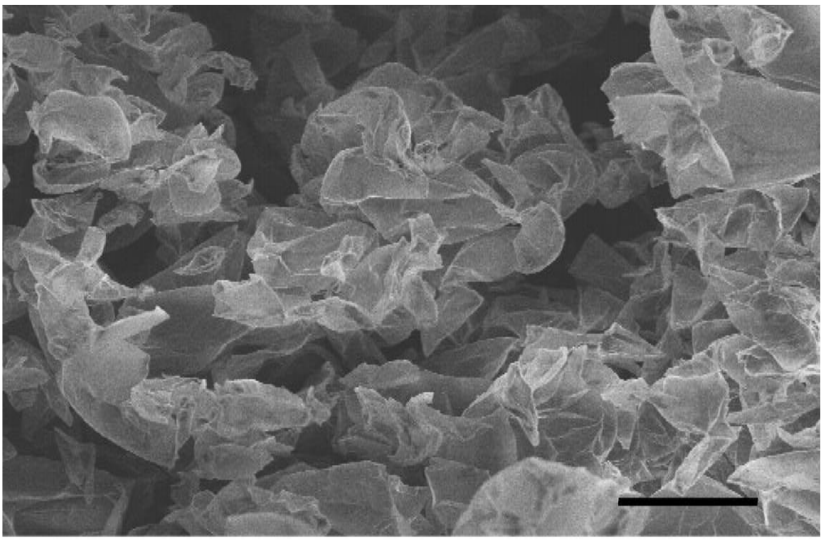

Figure 8: .Scanning electron microscopy image of curved graphene sheets (scale bar 10 μm) [Reprinted with permission from Ref. CITATION Che \l 1033 [6]. Copyright (2010) American Chemical Society.]

Liu et al. [6] developed mesoporous graphene electrode (made of graphene, mixed with 5 wt% Super-P and 10 wt% polytetrafluoroethylene (PTFE) binder) which displayed remarkably high EDL capacitance (154.1 F/g) and energy density (90 Wh/kg) at a current density of 1 A/g. The scanning electron microscopy image of the obtained graphene sheet is shown in Fig.8.

Fan et al. [35] reported an easy, cost-effective and environmentally friendly process for the large-scale synthesis of porous graphene nanosheets. The etching of graphene sheets by MnO_2 attained the porous structure. The open layered and mesoporous structure of electrode material found to facilitate efficient access of electrolyte and shorten the ion diffusion pathway. It displayed a specific capacitance of 154F/g at 500mV/s in 6M KOH electrolyte and good cycle stability with only 12% of capacitance loss after 5000cycles.

Through the facile restraining-then-releasing approach in a greatly controlled mode, Xu et al. [36] fabricated transparent and stretchable SC from extremely thin buckled four-layer chemical vapour deposition (CVD) graphene films. The material shows 17.3 F /g specific capacitance with 98% capacitance retention after 10000 cycles in H_2SO_4-PVA gel electrolyte.

4.2. Doped Graphene

It is desirable to substitute a carbon atom in a graphitic lattice with a heteroatom to attain the exclusive properties expected for SC electrodes. Heteroatom-doped graphitic structures exhibit an improvement in energy density by generating active sites on the graphene surface. The heteroatom-doped graphene is obtained either by in situ processing or by the treatment with a heteroatom-containing precursor. The former performs during the synthesis of carbon material and the latter is the post-processing of carbon [37, 38].

4.2.1. Nitrogen-Doped Graphene

The modified electronic structure of N-doped graphene provides an increment in the capacitive property and the charge carrier density. The thermal annealing of GO and wet-chemical techniques are the most common heteroatom doping procedures. The type of synthesis determines the layer distribution of N-doped graphene. Mostly GO serves as the precursor in the post-processing methods to obtain doped graphene [37]. The SEM images of graphene aerogels developed by Sui et al. [39] is shown below. In the Fig.9. (a, b), the interrelated porous network of NGA which is composed of randomly oriented graphene sheets is demonstrated. The SC developed by the material offered a specific capacitance of 223F/g at 0.2 A/g and long-term cyclic performance.

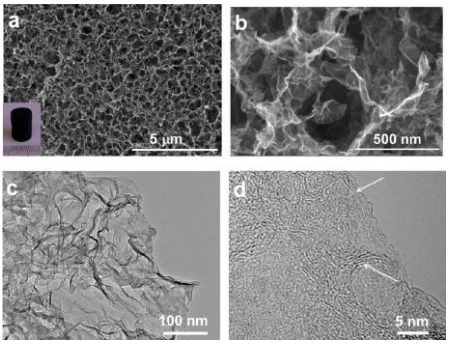

Figure 9: (a, b) SEM images of nitrogen-doped graphene aerogel at different magnifications; (c, d) TEM images of NGA at different magnifications. Inset: a digital photo of the NGA. [Reprinted with permission from Ref. CITATION Zhu15 \l 1033 [39] Copyright (2015) American Chemical Society.]

Liu et al. [40] Prepared three-dimensional porous nitrogen-doped graphene hydrogel via simple one-step hydrothermal reduction with GO and ammonium bicarbonate. The SC with the material as electrode showed enhanced performance with a specific capacitance of 48.6 F/ g and high energy density of 94.5Wh/ kg. The material displayed a 3D porous structure with a large surface area. Nitrogen doping enhanced electrochemical performance and the overall capacitance by enabling fast ion mobility and improved conductivity.

Peng et al. [41] synthesised highly crumpled Nitrogen-doped graphene-like nanosheets with high specific surface area by a simple pyrolysis process. Urea and $CaCl_2$ were used as nitrogen source an activating agent respectively. The product material exhibits good cyclic stability and a specific capacitance of 226 F/g in 6M aqueous KOH with energy and power densities of 17.0 Wh/ kg and 225 W/kg respectively.

4.2.2. Boron-Doped Graphene

Doping into a graphene lattice boosts the specific capacitance and induces a remarkable enhancement in SC performance. It is amenable to substitute carbon atoms by Boron as it consists of one electron less than the carbon atom. The Boron atom generates sp^2 hybridisations by way of acting as a p-type dopant in the carbon lattice. The substitutional reaction of boron oxide, laser ablation technique, arc discharge, hydrothermal treatment, chemical vapour deposition and so on are the general methods to prepare Boron doped graphene [42].

Niu et al. [43] followed the pyrolysis of GO with boric acid (H_3BO_3) in an argon gas atmosphere at 900^0C. After 3 hours of pyrolysis, the boron content increased to the highest value of 4.7%. The incorporation of Boron atoms and the presence of oxygen atoms in the resultant material creates an increment in the capacitance (172.5 F/ g at 0.5Ag) and cycling stability (96.5% of initial capacitance after 5000 times of cycling) with a high energy and power density (3.86Wh/ kg and 125W/kg respectively). Chen et al. [44] reported a controlled synthesis of the nitrogen-doped graphene hydrogel trough hydrothermal process that is favourable for mass production of nitrogen-doped graphene hydrogel. The organic

amine works as a nitrogen source and it adjusts the Inner structure of the material. The SC performance of the material is appreciable with a high power density of 205.0 kW/kg and 95.2% of its capacitance retention after 4000 cycles.

4.2.3. Boron and Nitrogen Co-doped graphene

Graphene possesses a semi-metal nature with zero band-gap. The doping of graphene with Boron and Nitrogen atoms opens the band-gap of graphene and generate new properties which can effectively enhance the specific capacitance and improve the durability of SC electrodes. The improvement in the electrochemical performance attributed to the carbon networks that facilitate the charge transfer between the neighbouring carbon atoms [45, 46].

Using GO and ammonia boron difluoride (NH_3BF_3) as precursors Wu et al. [46] synthesised Boron and Nitrogen co-doped graphene aerogels through the hydrothermal reaction and freeze-drying processes. The resultant 3D interconnected frameworks showed a macroporous architecture that is favourable for the ion diffusion process and the electron transport in the bulk electrode. The material subjected to physical pressing to process thin electrode plates offered a high specific capacitance (62 F/ g) and enhanced energy density (8.65 W h /kg) at high power density (1600 W/ kg).

Boron and nitrogen co-doped graphene-like carbon (BNC) with a gram scale synthesised by Chen et al. [47] exhibited a specific capacitance of 225 F/g at 0.25 A/g in 6 M KOH electrolyte and high cycling stability with 93% capacitance retention over 20000 cycles. The device could deliver an energy density of 5.3 Wh/kg at a high-power density of 30 kW/kg. The two-step synthesis includes a ball-milling process that generates high surface area with abundant active sites followed by a calcination process.

4.2.4. Phosphorus-Doped Graphene

The larger atomic size and lower electro-negativity of Phosphorus can form structural distortion defect-induced active surface when it doped to the graphene [48]. Due to the increased electrical conductivity and the pseudocapacitance, the phosphorus-doped graphene exhibits an enhanced capacitive performance. Karthika et

al. [49] have achieved the synthesis of phosphorous-doped graphene from rGO sheet for which the electrochemical measurements showed a high specific capacitance of 367 F/g with energy density and power density of 9kW/kg and 59Wh/kg respectively. There was no degradation of the electrodes up to 5000 cycles indicating very high cyclic stability. By the annealing of graphene and phosphoric acid mixture Wen et al. [50] employed the synthesis of Phosphorus-doped graphene with a P doping level of 1.30 at%. The SC assembled using the material delivers a high energy density of 11.64 Wh/kg and a high-power density of 831 W/kg and offers 3% performance degradation after 5000 cycles.

4.3. Graphene-based Fibres

Graphene-based fibres have received immense attention for their outstanding electrical conductivity, enhanced mechanical strength and excellent flexibility conductivity compared to the two-dimensional and three-dimensional forms of graphene. Their porous structure provides a considerable increase in the specific capacitance as they are used as SC electrodes. Mostly, the synthesis process followed is the wet-spinning process. The introduction of metal oxides, hydroxides and conducting polymers offer a desired pseudo-capacitance to the material while graphene acts as a conductive channel [21, 8, 51].

The rGO fibre-based springs designed by Wang et al. [52] displayed a volumetric capacitance of 25.9 F/ cm^3 in a PVA-H_3PO_4 gel electrolyte. The RGO-based fibre wires consisting of polypyrrole -decorated RGO/multiwalled carbon nanotubes (PPy/ RGO/ MWCNT) were obtained by injecting the mixture solution of the materials into pipes having a diameter of 1.5 mm. The microstructure of the obtained fibres is shown in Fig.10. The SC assembled with the fibres showed a high energy density of 0.94 mWh/ cm^3 at a power density of 7.32 mW/cm^3 along with 82.4% capacitance retention after a large stretch (100%), and 54.2% capacitance retention after the third healing.

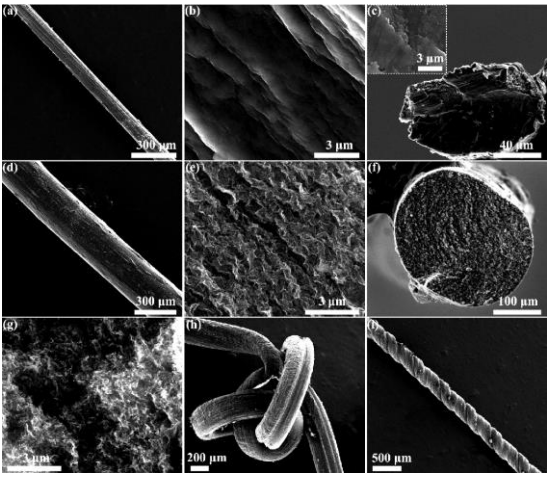

Figure.10. Microstructure of RGO-based fibre. (a, b) Side view and (c) cross-sectional SEM images of the RGO fiber, (d, e) side view and (f,g) cross-sectional SEM images of the RGO/MWCNT fiber with an initial weight ratio of 1:1 at low and high magnifications, respectively. SEM images of a (h) knotted and (i) twisted RGO/MWCNT fibers. [Reprinted with permission from Ref. CITATION Sil17 \l 1033 [52] Copyright (2017) American Chemical Society.]

Chen et al. [53] proposed solid-state SCs assembled from NLC-R1.0 RGO fibres, which exhibits specific capacitance of 279 F/ g. They followed a scalable non-liquid-crystal spinning process for the production of continuous graphene fibres with tailored structure.

The fibre SCs based on the hollow composite fibre fabricated by Qu et al. [54] revealed an excellent specific capacitance of 304.5 mF/cm^2. The energy densities based on the single fibre electrode is 27.1 µW h/cm^2. The electrochemical performances found to be well maintained after bending for 500 times. 96% of capacitance retained after 10000 cycles. Yang et al. [55] developed a fibre-shaped SC by winding aligned CNT sheets on elastic fibres. The highly stretchable device exhibited a specific capacitance of 20 F/g in H_3PO_4–PVA gel electrolyte. An energy density of 0.515 Wh/kg obtained at a power density of 421 W/kg. 90% capacitance of the device retained after 1000 charge-discharge cycles when applied a strain of 75%. Li et al. [56] reported a simple technique to synthesis graphene fibre derived from chemical vapour deposition grown graphene films. Graphene is an organic solvent like ethanol or acetone is allowed to self-assemble from a 2D film to a fibre structure. Once it dried, the sample attains a porous and crumpled

form. The fibres having 20 -50µm thickness showed capacitance values ranging from 0.6 to 1.4 mF/cm^2 with good cyclic stability.

4.4. Graphene-based nanoribbons

Graphene nanoribbon (GNR), the thin and elongated form of graphene shows either semiconductor or semimetal characteristics based on its width and edge properties. Electron beam lithography, physical and chemical methods, splitting of carbon nanotubes, chemical vapour deposition and so on are some of the common methods to develop GNRs. The major challenge of the area is controlling the widths and lengths of the GNRs. Mostly, the edge-opened GNRs seem to be more susceptible to defects than carbon nanotubes [57].

Shi et al. [58] reported a facile method for the synthesis of rGO micro ribbons through photochemical reduction mechanism of self-assembled GO liquid crystals. The obtained material possesses tunable diameters and can be tailored into desired geometries such that it could be used as textile electrodes for micro SCs. The device showed high areal specific capacitance of 14.4 mF/cm^2 and outstanding cycling performance (96.8% capacitance retained after 10000 cycles). The microstructure of the sample is shown in Fig.11

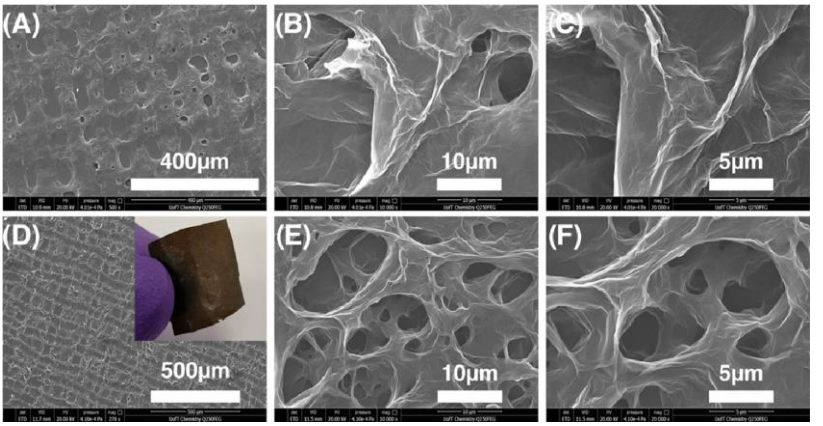

Figure.11: Scanning Electron Microscopy (SEM) images and a digital photograph of the crisscross rGO-MR textiles washed with different liquids.

(A−C) Crisscross-patterned rGO-MR films washed with distilled water. (D−F) Crisscross-patterned rGO-MR films washed with ethanol. Inset: Freestanding crisscross rGO-MR film extracted from the solution surface. [Reprinted with permission from Ref. CITATION Hao19 \l 1033 [58] Copyright (2019) American Chemical Society.]

Sharma et al. [59] synthesised supercapacitor electrodes with graphene oxide nanoribbons (GONR) & reduced graphene oxide nanoribbons (RGONR) supported polyaniline (PANI) nanocomposites through in-situ chemical polymerisation approach. The device exhibits better electrical and electrochemical properties of GONR/RGONR supported PANI nanocomposites because of the synergistic impact of GONR/RGONR and PANI. Moreover, asymmetric devices are fabricated using GONR/RGONR as negative electrode while GONR/PANI and RGONR/PANI as positive electrode show off considerable enhancement in energy density and device overall performance. Each of the nanocomposites owns more suitable specific capacitance (specific capacitance as 740 F/g for GONR/PANI & 1180 F/g for RGONR/ PANI at 5 mV/s).

Sahu et al. [60] unzipped the MWCNTs chemically to obtain lacey rGO nanoribbon (LRGONR) using a strong oxidising agent The obtained nanoribbons showed enhanced electrolytic accessibility and de-stacking property for all the layers of graphene. The controlled reaction of opened MWCNT with different oxidisers exaggerate the defects and edge sites in rGO nanoribbon by creating holes and defects. Through the reduction of GO with malonic acid, the SC cell developed with the material showed outstanding energy and power density values exhibited by the material in an aqueous electrolyte of 15.06 Wh/kg and 807 W/kg respectively at 1.7 A/g. In non-aqueous electrolyte, the values are 90 Wh/kg and 2046.8 W/kg respectively at 1.8 A/g.

Khandelwal et al. [61] employed a chemically controlled nucleation and growth of graphene for the synthesis of GNRs with high conductivity at a low PH value (6.0). The higher PH values (8-11) and a higher concentration of malonic acid results in the formation of nano-sheets. The material possesses good cyclic stability for 4000 charge-discharge cycles at 15 A/g with appreciable energy

density/power density (16.84 Wh/kg / 5944 W/kg) and specific capacitance (301 F/g at 1 A/g)

4.5. Graphene-Based Composites

The hybridisation of graphene powder with conductive polymers and metal oxides prevents the restacking process and improves the overall performance by the addition of pseudocapacitance [20, 8]. The exfoliated single layer of graphene composite shows an improvement in thermal conductivity, mechanical stability, electrical conductivity and surface area [62].

4.5.1 Graphene-Based Polymer Composites

Graphene-based polymer composites fabricate by the nano level dispersion of graphene particles in a polymer matrix. The upgrading of thermal, mechanical and electrical properties of graphene-based polymer composites depends on the properties of graphene and the polymer matrix. A pure form of graphene is incompatible with organic polymers [62].

The report published by Xiang et al. [63] proposed a facile and environmentally friendly process for synthesising three-dimensional rGO through a single-step hydrothermal strategy. Glucose served as reducing agent and $CaCO_3$ as the template. The device exhibits specific capacitance of 1586 F/g. Chen et al proposed a facile co-electrodeposition process [64] to design reduced graphene oxide/polypyrrole (rGO/PPy) composite films, which provides a specific capacitance of 361 F/g. They used sodium dodecylbenzene as both a surfactant and supporting electrolyte in the precursor solution.

An effective way for the synthesis of a graphene-single-walled carbon nano tube-poly (3-methyl thiophene) ternary nanocomposite was reported by Dhibar et al. [65] that has found to be a potential candidate for supercapacitor electrode with a maximum specific capacitance of 561F/g. The device offers a high energy density (48.97 W h/kg) and a high-power density (1579.35 W/kg) along with better thermal balance and advanced electrical conductivity.

Zhang et al. [66] designed a hybrid conductive hydrogel showing excellent SC performance using a specific water-soluble copolymer

using a central poly(ethylene oxide) block, terminal poly(acrylamide) and aniline moieties randomly incorporated developed by reversible additional fragment transfer polymerisation. The flexible SC based on this hybrid hydrogel electrode presents a specific capacitance of 187 F/g and cyclic stability with 90% capacitance retention after 1000 cycles.

4.5.2. Graphene-Based Metal Oxide Composite

Jiang et al. [67] synthesised flexible nanohybrid paper electrode based on full inkjet printing synthesis of a freestanding graphene paper (GP) 3D porous graphene hydrogel (GH) − polyaniline (PANI) nanocomposite. The SC assembled using the material exhibits amazing flexibility and appreciable energy density of 24.02 Wh/kg at a power density of 400.33 W/ kg. The microstructure of the obtained composite is given in Fig.13.

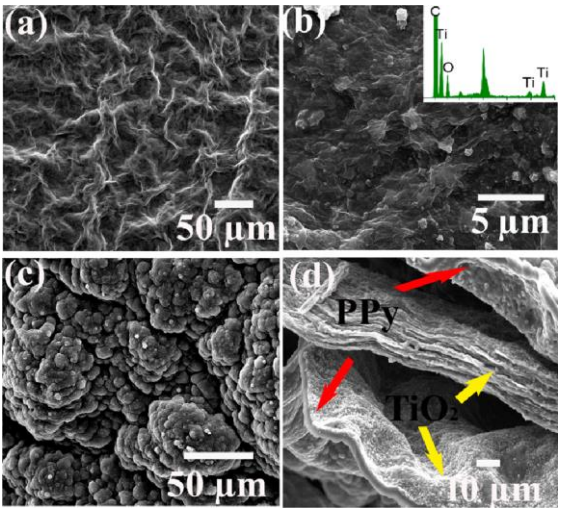

Figure.13. SEM micrographs of graphene-based films. (a) G films; (b)TiO_2−G composite films with the EDS spectra of TiO_2−G composite film as an inset; (c) TiO_2−G−PPy composite films; (d) the cross-section of TiO_2−G−PPy. Red arrows marked the PPy coating, and yellow arrows marked TiO2 nanoparticles. [Reprinted with permission from Ref. [67] Copyright (2015) American Chemical Society.]

Halder et al. [68] designed an asymmetric SC using 3Dquaternary mesoporous Cu−Ni−Ce−Co oxide nanoflakes through a single-step hydrothermal protocol followed by heat treatment. The SC assembled by the material in KOH electrolyte provides a specific capacitance of 183.3 F/ g and an energy density of 51Wh/ kg at a

power density of 581.9W/kg. The device possesses high cyclic stability. Kumar et al. [69] followed a facile inexpensive method to develop 3D self-assembled hierarchical nanostructure Co3O4 nanobeads-CNTs-GNSS, which in a KOH electrolyte exhibits a maximum specific capacitance of 600F/g. The CoMn2O4/3DrGO heterostructure fabricated by Zhang et al. [70] shows 1028 F/ g specific capacitance in 6 M KOH aqueous solution. The device shows excellent stability in an extended potential window of 1.8V. Cheng et al. [71] achieved a template fabrication of amorphous Co2SiO4 Nanobelts/Graphene Oxide Composites with an areal capacitance of 229 mF/ cm2 in 3 M KOH aqueous electrolyte.

The SC electrodes developed by Wu et al. [72] showed a specific capacitance of 467.2F/g in Na_2SO4/PV electrolyte. They designed self-standing $MnCO_3$@graphene/CNT film electrodes by a one-pot hydrothermal process for the encapsulation of $MnCO_3$ in graphene nanosheet, in which each $MnCO_3$ nanorod enveloped by graphene. The chlorine-doped reduced graphene oxide films (Cl-RGOFs) fabricated by Jiang et al. [73] exhibits 210 F/g in KOH-PVA gel electrolyte. They chose a facile hydrochloric acid solvothermal process to prepare chlorine-doped reduced graphene oxide films.

4.6. Graphene sponge, Aerogel

The 3D forms of graphene such as foams, sponge, network, aerogels, hydrogels and so on preserve the graphene sheets from re-stacking effect. They also provide three-dimensional channels for the rapid transport of electrons formed by the inter-related pores [20].

Xu et al. [74] introduced a sponge-like graphene structure through the microwave synthesis and carbonisation of cobalt phthalocyanine molecules. The product displayed specific capacitance of 53 F/g at 100 A/g. The energy density and power density delivered by the device is 7.1 Wh/kg and 48000 W/kg. Fig.14. below shows the microstructure of 3D sponge synthesised by the team.

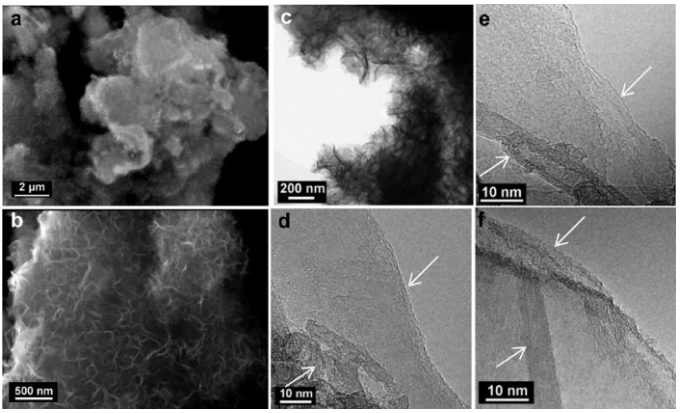

Figure.14. (a, b) SEM micrographs of the 3D SPG. (c) TEM, and (d,e,f) HRTEM micrographs of the 3D SPG. [Reprinted with permission from Ref. [74] Copyright (2012) American Chemical Society.]

Chen et al. [75] developed a hierarchical mesoporous VO_2/graphene@NiS_2 hybrid aerogel via sol-gel and hydrothermal growth. In PVA/KOH gel electrolyte, the specific capacitance of the device is 1280.0 F g-1. The freestanding conductive MoS_2 hydrogel designed by Liu et.al [76] provides 160 F/ g specific capacitance in 1.0 M H_2SO_4 electrolyte. The 3D nitrogen-doped graphene sponge (NG) synthesised by Elessawy et al. [77] exhibited an outstanding performance as SC electrodes. The material is derived from waste polyethene terephthalate (PET) bottles cost-effectively. Through a one-step process, PET mixed with urea at diverse temperatures and the obtained NG showed a maximum specific capacitance of 405 F/ g in 6 M KOH.

The 3D graphene sponge prepared by Wan et al. [78] showed excellent conductivity. The material synthesised by a process in which a colloidal dispersion of GO has derived from oxidised natural graphite powder through the modified Hummer method. The thick dispersion solution then freeze-dried for a single day to obtain GO sponge. The product material may be used as a reachable huge channel and large mass loading of a flexible conductive substrate for the growth of $NiCo_2S_4$ nanotube @Ni-Mn LDH arrays. The electrically conductive $NiCo_2S_4$ nanotube displays remarkable pseudo-capacitance and can act as an amazing conductive support for the overall performance Ni-Mn layered

double hydroxide (LDH). The specific capacitance offered by 3D $NiCo_2S_4$@Ni-Mn LDH/GS is 1740 mF/ cm^2 at 1mA/cm^2.

4.7. Graphene from Natural Sources

The soluble graphene from eucalyptus polyphenol solution introduced by Manchala et al. exhibits specific capacitance of 239 F/ g. They used a low-cost method to synthesis graphene with excellent deduction of oxygen functionalities. Li et al. [79] prepared a 3D porous carbon nanosheet via one-pot activation of forestry with copper bromide ($CuBr_2$). The obtained highly porous material in 1.0 M Na_2SO_4 offers a specific capacitance of 230 F/ g at 0.5 A/ g. Mangisetti et al. [80] followed a facile approach for the synthesis of N-doped two-dimensional wrinkled few-layered porous graphene nanosheets (N-HGNSs) from a bio waste material- Bombax malabaricum. The device exhibits 523 F/g specific capacitance in Na Cl-agarose solid-state gel electrolyte.

Chen and co-workers [81] used konjac glucomannan and graphene oxide as the carbon precursors develop ultra-light carbon aerogel from the Thalia dealbata stem. The resultant material possesses outstanding electrical conductivity, elasticity, cycle stability and specific capacitance of 287.6 F/g. Hekmat et al. [82] followed the one-step in-situ polymerisation technique to develop MnO2/PANI nanocomposite (MPNC) on a macroporous cellulose fibre network based current collector. A two-dimensional (2D) rGO sheet-based anode was prepared by vacuum filtration step followed by a freeze-drying process. The MPNC electrode designed through this simple and cost-effective process showed a notable specific capacitance of 190 F/ g and 87% capacitance retention after 1000 charge-discharge cycle. Nanaji et al. [83] reported a simple procedure to design nonporous graphene sheets from bio-waste. The activation temperature is used to tune the ratio between graphene like nonporous carbon structure and the amorphous carbon. With the increasing activation temperature, a stable graphene structure is derived from the amorphous carbon, which possesses a very high specific surface area. The SC assembled with the electrode material exhibited a specific capacitance of 282 F/g and an excellent cyclic performance. The energy and power

densities delivered by the device are 20.6 W h/ kg at 33,600 W/ kg. Fig.15. shows the schematic of the process followed by the group.

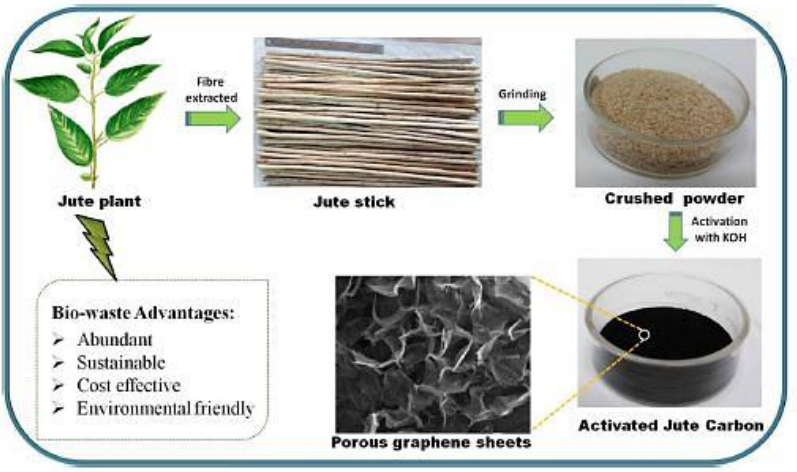

Figure.15. Production of graphene from the jute plant. [Reprinted with permission from Ref. [83] Copyright (2018) American Chemical Society.]

The Table below provides a comparison between the capacitive performances of various electrode materials.

Table 1: Performance of supercapacitors with different graphene-based materials

Sl. No	Material	Electrolyte	Maximum specific capacitance	Maximum energy density	Maximum power density	Cycling stability	Reference
1.	Solid-state Super capacitors assembled from NLC-R1.0-RGO fibres	1 M H_2SO_4	279 F/ g	5.76 Wh/ kg	47.3 W/ kg	92% after 1000 cycles	[53]
2.	Wide graphene nanoribbons (GNRs) by reduction of graphene	1M H_2SO_4	301 F/g	16.84 Wh/ kg	5944 W /kg	For 4000 cycles, at 15 A/g, 100%ef	[61]

	oxide (GO)					ficienc y	
3.	Lacey reduced graphene oxide nanoribbons (LRGONR)	2.0M H_2SO_4	1042 F/g	15.06 Wh/k g	807 W/ kg	97% after 3000 Cycles	[59]
		1.0 M TEA BF_4	1272 F/ g	90 Wh/ kg	2046.8 W/ kg	96.2% after 3000 cycles	
		1.0M BMIM BF_4/AN	1324 F/g	181.5W h/kg	2316.8 W/kg	96.6% after 3000 cycles	
4.	GONR-PANI Nano ribbons	1 M H_2SO_4	740 F/g	99.87 Wh/k g	1259 W/kg	85% retenti on after 2000 cycles	[59]
	RGONR-PANI Nano ribbons		1180 F/g	166 Wh/k g	3292 W/kg	90% retenti on after 2000 cycles	
5.	Chlorine-doped reduced graphene oxide films (Cl-RGOFs)	KOH-PVA gel electrol yte	210 F/g at 1 A/g	160.6 Wh/c m^2	0.5m W/cm^2	98% after 500-time mecha nical bendin g	[73]
6.	Boron-doped graphene	6 M KOH	172.5 F/g	3.86 Wh/k g	125W/ kg	96.5% after 5000 times of cycling	[43]
7.	Boron and Nitrogen co-doped graphene aerogels	polyvin yl alcohol (PVA)/ H_2SO_4 gel	62 F/g	8.65 Wh/k g	1600 W/kg	Excelle nt cycling stabilit y ≈ 100%	[46]

8.	Boron and nitrogen co-doped graphene-like carbon (BNC)	6 M KOH	225 F/g	5.3 Wh/kg	30 kW/kg.	93% capacitance retention over 20000 cycles	[47]
9.	phosphorous-doped graphene from rGO sheet	1M H_2SO_4	367 F/g	59 Wh/kg	9 kW/kg	No degradation of the electrodes up to 5000 cycles	[49]
10.	Phosphorous doped graphene nanosheets by the activation with phosphoric acid	1 M H_2SO_4	115 F/g	11.64 Wh/kg	831 W/kg	3 % performance degradation after 5000 cycles	[71]
11.	Nitrogen-doped graphene hydrogel	5 M KOH	92 F/g	3.2 Wh/kg	253 kW/kg	95.2% of initial capacitance was retained for 4000 cycles	[44]
12.	3D porous nitrogen-doped graphene hydrogel	[BMIM] PF_6 electrolyte	48.6 F/g	92.5 Wh/kg	640 W/kg	13% after 5000 cycles	[40]
13.	Nitrogen-doped activated carbon derived from prawn shells	1 M H_2SO_4	695 F/ g	10 Wh/kg	1000 W/ kg	stable cycle life over 5000 cycles	[84]
	Nickel-based	357 F/g	6MKOH	59	900		

14.	pillared MOF (DMOF-ADC) and rGO, denoted as ADC-rGO			Wh/kg	kW/kg	95% after 10000 cycles	[85]
15.	Highly crumpled nitrogen-doped graphene-like nanosheets	6M aqueous KOH	226 F/g	17.0 Wh/kg	225 W/kg	97% capacitance retention after 5000 cycles	[41]
16.	Ag−Ni Nanoparticle Anchored Reduced Graphene Oxide Nanocomposite	3 M KOH electrolyte	897 F/ g At 1 A/g	80 Wh/ kg	400 W/kg	77% after 4000 cycles.	[86]
17.	ZIF-67 and rGO comp99osite	0.2M $K_3[Fe(CN)_6]$ in 1 M Na_2SO_4	1453 F/ g at 3 A/ g	25.5 Wh / kg	2.7 kW/ kg	88% after 1000 cycles	[87]
18.	$MnCO_3$@graphene/CNT hybrid film	Na_2SO_4 / PV electrolyte	467.2F/ g	27 Wh/ kg	271.7 W/kg	93% after 6000 cycles	[72]
19.	Copper ferrite nanoparticle-attached graphene nanosheet ($CuFe_2O_4$-GN)	3M aqueous KOH solution	720 F/g	15.8 Wh/ kg	1.1 kW/ kg	85% capacitance retention after 1000 cycles	[88]
20.	3D hierarchical graphitic carbon nanocomposites with	6 M KOH	1586 F/g At current density 1.0 A/g	54.7 Wh /kg	748.6 W/ kg	94.5% after 10000 cycles	[63]

	highly dispersed mixed (Co-Ni-O/3DG)						
21.	$CoMn_2O_4$/ 3DrGO hetero Structure	6M KOH aqueous solution	1028 F/ g	46.35Wh/kg	900 kW/ kg	89.7% after 5000 cycles	[70]
22.	VO_2/ graphene@NiS_2 hybrid aerogel electrode	PVA/ KOH gel	1280.0 F/ g	60.2 Wh/ kg	350.0 W/ kg	86.2% after 10,000 cycles	[75]
23.	Free standing conductive MoS_2 hydrogel	1.0 M H_2SO_4	160 F/ g	3.4 Wh/kg	7.0×10^4 W/kg	90% after 5000 cycles	[76]
24.	3D sponge-like graphene nano architectures	1 M H_2SO_4	53 F/g at 100 A/g.	7.1 Wh/kg	48000 W/kg	98% after 10 000 cycles	[74]
25.	3D sponge nitrogen doped graphene	6 M KOH	405 F/ g	68.1 Wh/kg	558.5 W /kg	87.7% after 5000 cycles	[77]
26.	Micro dome-like graphene by CVD	PVA/H_3PO_4 electrolyte	293 F/g	63.6 Wh/kg	1261 W/kg	96.5% after 10000 cycles	[89]
27.	High-Performance Layer-by-Layer Self-Assembly PANI/GQD-rGO/ CFC	H_2SO_4/ PVA gel	1036 F/ g	30.6 Wh/kg	2118.5 W/kg	97.7% after 10000 cycles	[90]
28.	Nano cellulose/ RGO/in Situ Formed PANI	1 M sulfuric acid	79.71 132 F/ g	5.09 Wh/ kg	147.53 W/kg	84.8% after 1000 cycles	[91]
	Gr			48.97	1579.35	93%	

29.	SWCNTs−PMT ternary nanocomposite	1 M KCl	561F/g	Wh/kg	W/kg	after 1000 cycles	[65]
30.	Bark-Based 3D Porous Carbon Nanosheet	1M Na_2SO_4	230 F/ g	24.3 Wh/kg	224.9 W/kg	98.3% after 10000 cycles	[79]
31.	MPNCs @cellulose//rGO@ cellulose-based ASC	1M H_2SO_4 aqueous electrolyte	103 F/ g	41.5Wh/ kg	491 W/kg	78% after 3000 cycles	[82]
32.	Nanoporous Graphene Sheets from Bio-waste	6M KOH	282 F/g	20.6 Wh/kg	33600 W/kg	70% at high current rates	[83]

5. Challenges and Future Prospects of Graphene-Based Supercapacitors

The efficient alterations and modifications made in graphene-based materials extremely enhanced their performance as SC electrodes. The 3D graphene structures and their composite forms explore in energy storage applications but their large-scale cost-effective production for commercial demands still has to meet. Hence, the forthcoming researches should focus on designing the 3D structures of graphene. The GO, which is the basic precursor for most of the fabrication technique, is costly and the environmentally friendly strategies have to be promoted for material development. To realise the unlimited applications of graphene in SC technology the quality of electrode materials still has to improve [92].

The fields of production and characterisation of graphene, the fabrication of SC with graphene materials etc. has to improve to overcome the challenges faced by graphene SCs. The chemical and thermal reduction of graphite into GO and the exfoliation graphene found to be a profitable method but, a major drop in the desirable properties of graphene raises challenges. So, controllable strategies are suggested for the production of high-quality graphene. The fast-rising of flexible and wearable electronics demands the progress of flexible, deformable SC electrodes. The optimisation of

efficient graphene-based flexible SCs joined with other energy devices (nano-generators, solar cells, and Lithium-ion batteries) has become a challenge and vital prospect. The improvement in the control of the interfacial interaction between graphene and pseudocapacitive materials has to attain to boost the overall Faradic processes across the interface. The mechanical flexibility of graphene-based materials will be of considerable interests for future researches [20].

6. Applications of Graphene as a Supercapacitor Material

Graphene is a highly attractive material, as its fundamental properties make it highly suitable for a broad range of applications in numerous fields. In the case of energy storage systems, graphene has a high surface area of 2675 m^2/g, which when applied to SCs as an electrode material, allows for an EDL capacitance of ~550 F g^{-1} given that maximum surface area is utilised [6, 93]. It has properties that make it a highly preferred material for SC applications such as fast charge and discharge, low internal resistance, high tolerance for extreme temperatures, absence of toxic chemicals and a very high number of charge-discharge cycles [93].

Thus, graphene has unique properties that enable the superiority of energy storage systems. However, while the potential for such applications is many, it is yet to be commercialised on a large scale for mass production, and hence is restricted to research and development. Nonetheless, with further investment, in time, graphene can be seen as a prospective material for many applications in the supercapacitor industry.

In the automotive sector, graphene could enable electric cars to operate on the same level as that of conventional fuels like petrol and still recharge in far lesser time of minutes. In time, graphene could be a critical component of batteries and SCs in cars to improve performance and efficiency, whilst reducing the power consumed. To achieve the proposed state, however, many factors come into play, some of which are unattainable due to lack of feasible techniques, inferior technology to achieve the desired level of efficiency of the graphene material.

Another notable example is that of a flexible 3-dimensional graphene foam-based material (GFSC) used in SC applications for smart energy systems implemented in portable energy applications such as wearable systems, defence and so on. Here, conventional Li-ion based batteries are not suitable as they, in comparison, have poor performance, are heavier and bulkier, and generate excess heat. GFSCs consisting of a novel layered structure of highly conductive electrodes (graphene-Ag conductive epoxy-graphene foam), has superior electrochemical and super capacitive performance, is lightweight, cost-effective in fabricating, does not self-heat, and are stable with up to 68% retention of capacitance after 25000 charge-discharge cycles. Possible applications can include those of health care monitoring such as e-skin, smart coatings, sensing patches or tattoos, or vehicles, robotics and prosthesis, which require higher energy sources and inputs [94].

Transportation can also be improved with, in many of its applications. The issue lies in trying to minimise the consumption of energy and CO_2 emissions. SCs can be implemented in Hybrid Electric Vehicles on matters of energy recovery, by harnessing regenerative energy during braking at stops and reusing the energy when accelerating, thus improving fuel efficiency. SCs are also capable of capturing and dissipating the heat generated from exothermic reactions and resistances [95]. Furthermore, the characteristic of quick charge-discharge cycles finds applications in capabuses or 'capacitor buses'. Developed in China, these type of buses utilise power stored in large onboard EDLCs without relying on conventional sources for power. The EDLCs can be recharged quickly at bus stops and fully charged at terminals. Over the years, demand in many countries has increased for such types of buses, as part of initiatives to opt for a greener and efficient means of transport [96, 97].

Industrial applications mainly rely on SCs as backup power sources due to their quick discharge power. This allows for implementation in scenarios where continuous power supply is a necessity such as in hospitals or critical computer memory components such as solid-state drives to prevent loss of data in case of a power cut. SCs have also been installed as arrays in the Airbus A380 in the actuators of emergency exit doors for immediate powering, are the main power

source in drills used in oil, petroleum or geothermal activities, due to its stability in extreme environments [95]. They have been used in tandem with batteries as a hybrid system, with applications as backup medical imaging equipment [95, 98]. Communication and information technology depend on SCs for modulation purposes, to control the intensity, phase or polarisation of light. While most SCs for this purpose are of the compound or semiconductor type, with the introduction of graphene, modulation efficiency is improved, allowing for applications in plasmonics and optoelectronics [99].

Military applications have also been able to incorporate SCs into their designs such as laser power supplies, radar antennae in the form of bursts of power to send signals, backup power systems for emergency airbag deployment, avionics display and instrumentation involving data backup and storage [100]. Initially deployed in tanks, submarines or vehicles with large engines as short-term power sources to cold start the engines with diesel fuels, or to provide emergency power to doors, various applications have come up over time. Notable examples are emergency power systems for data backup in robots and fire suppression systems in armoured vehicles and munition systems for the provision of short-term power in GPS-guided missiles and projectiles, tank gun turrets, and land-based launch systems. They are also applicable in RF systems, improving signal strength, and can be used as backup power for distress signals. When used in parallel with batteries, they are at their peak power, making them suitable portable military electronics [101].

Alternative energy sources such as windmills are also becoming more reliant on SCs than batteries. Popular advantages include low maintenance cost, long cycle life and sufficient short bursts of power to the turbines in quick response to unpredictable weather conditions [95]. Solar energy is also being harnessed and stored in the form of environment-friendly LED street lamps where the constituent solar panels capture the energy and store it in SCs during the days. At night, this energy is used in powering the lamps, thus contributing towards longer life and lesser maintenance for years [95]

Soon, with rising concerns of dependence on fossil fuels, there is an increasing emphasis on alternative sources that are more environment-friendly and emit less or no harmful byproducts. In the future, many devices and technologies should adhere to stricter environmental standards. Wearable devices are one of such examples, which will be of huge demand in future electronics. Here, major advantages that can be incorporated include that of flexibility, light-weightedness, compact sizes, and resistance to abrasions, cuts and damages. They can be designed in any shape, without compromising efficiency therefore can cater to versatile applications such as cloth, smart glasses or watches and other miniaturised device applications [102]. In matters of flexibility, there is a large demand for flexible energy storage devices with sufficient power density and output range whilst being compatible with wearable electronic devices such as human skin wearable power generators [103]. Ultra-thin graphene films can be used in SCs in transparent electronics due to their high mechanical strength and flexibility. Furthermore, graphene has a high solubility in several solvents making it suitable for printing on substrates for integration in printable electronics [104]. For clothing, flax-derived carbon cloth supported by manganese nanosheets (MnO_2) can exhibit advantages of high specific capacitance as electrode material aside from abundance and low cost [105]. There are also possibilities of laser-printed graphene SCs of dimensions of $100cm^2$ with additional characteristics of high-temperature tolerance, inexplosive nature, long-term energy storage, and stretchability of up to 200%. These self-reliant on-chip units can be an integral part of future electronic and optoelectronic textiles [106].

7. Conclusion

Graphene in its different forms and structures is widely used as electrode materials in SCs due to its unique physical, chemical and mechanical properties. Among the various structures of graphene, the 3D forms explore with the availability of active sites and several possible ways to enhance the conducting routes and surface area. The production of graphene from natural sources opened cost-effective production processes for SC electrodes. The emergence of flexible graphene-based electrodes boosts the area of flexible and

wearable electronics. The hybrid combinations are favourable for high power and energy density applications. Groundbreaking research efforts have been done to modify the structure and upgrade the overall performance of the SC device and to reduce the production cost. The re-stacking effect of graphene layers is manageable by the facile methods and the stabilisation of graphene in different solvents. The addition of metal oxides conducting polymers helps to improve the capacitance. The graphene-based fibres and thin graphene-based films show excellent flexible and conductive properties. The 3D structures of graphene ensure effective power performance by preventing the agglomeration process and improving the stability of graphene.

References

[1] Y. Wang, Z. Shi, Y. Huang, Y. Ma, C. Wang, M. Chen and Y. Chen, "Supercapacitor Devices Based on Graphene Materials," *The Journal of Physical Chemistry,* no. 113(30), pp. 13103-13107, 2013.

[2] W. Raza, F. Ali, N. Raza, Y. Luo, K.-H. Kim, J. Yang, S. Kumar, A. Mehmood and E. E. Kwon, "Recent advancements in supercapacitor technology," *Nano Energy,* vol. 52, pp. 441-473, 2018.

[3] AZoNano, "What is an Ultracapacitor?," 6 7 2012. [Online]. Available: http://azonano.com/article.aspx?ArticleID=3044. [Accessed 23 11 2019].

[4] Wikipedia Contributors, "Supercapacitor," 18 11 2018. [Online]. Available: https:// en.wikipedia.org/ wiki/ Supercapacitor # Energy_recovery. [Accessed 23 11 2019].

[5] A. Borenstein, O. Hanna, R. Attias, S. Luski, T. Brousse and D. Aurbach, "Carbon-based composite materials for supercapacitor electrodes: a review," *Journal of Materials Chemistry A,* vol. 5, no. 25, pp. 12653-12672, 2017.

[6] C. Liu, Z. Yu, D. Neff, A. Zhamu and B. Z. Jang, "Graphene-Based Supercapacitor with an Ultrahigh Energy Density," *Nano Letters,* vol. 10, no. 12, pp. 4863-4868, 2010.

[7] X. Zhang, H. Zhang, C. Li, K. Wang, X. Sun and Y. Ma, "Recent advances in porous graphene materials for supercapacitor applications," *RSC Adv.,* vol. 4, no. 86, pp. 45862-45884, 2014.

[8] Q. Ke and J. Wang, "Graphene-Based Materials for Supercapacitor Electrodes – A Review," *Journal of Materiomics,* vol. 2, no. 1, pp. 37-54, 2016.

[9] C.-F. Liu, Y.-C. Liu, T.-Y. Yi and C.-C. Hu, "Carbon materials for

high-voltage supercapacitors," *Carbon,* vol. 145, pp. 529-548, 2019.

[10] X. Zhang, H. Zhang, C. Li, K. Wang, X. Sun and Y. Ma, "A Review of Supercapacitor Modeling, Estimation, and Applications: A Control/Management Perspective," *RSC Adv.,* vol. 4, no. 86, pp. 45862-45884, 2014.

[11] E. Goikolea and R. Mysyk, "Nanotechnology in Electrochemical Capacitors," in *Emerging Nanotechnologies in Rechargeable Energy Storage Systems*, 2017, pp. 131-169.

[12] H. Wang and L. Pilon, "Accurate Simulations of Electric Double Layer Capacitance of Ultramicroelectrodes," *The Journal of Physical Chemistry C,* vol. 115, no. 33, pp. 16711-16719, 2011.

[13] A. Velikonja, E. Gongadze, V. Kralj-Iglič and A. Iglič, "Charge Dependent Capacitance of Stern Layer and Capacitance of Electrode/Electrolyte Interface," *International Journal of Electrochemical Science,* vol. 9, pp. 5885 - 5894, 2014.

[14] P. Simon and Y. Gogotsi, "Materials for Electrochemical Capacitors," *Nature Materials,* vol. 7, no. 11, pp. 845-854, 2008.

[15] E. Esther, Y. Hua and H. H. Tezel, "Materials for Energy storage: Review of Electrode Materials and Methods of Increasing Capacitance for Supercapacitors," *Journal of Energy Storage,* vol. 20, pp. 30-40, 2018.

[16] P. Ratajczak, M. E. Suss, F. Kaasik and F. Béguin, "Carbon electrodes for capacitive technologies," *Energy Storage Materials,* vol. 16, pp. 126-145, 2019.

[17] B. E. Conway, "Electrochemical Capacitors Based on Pseudocapacitance, " *Electrochemical Supercapacitors* , pp. 221-257, 1999.

[18] "Intercalation / Deintercalation," 2019. [Online]. Available: https://www.fkf.mpg.de/133111/De_Intercalation.

[19] V. Augustyn, P. Simon and B. Dunn, "Pseudocapacitive oxide materials for high-rate electrochemical energy storage," *Energy & Environmental Science,* vol. 7, no. 5, p. 1597, 2014.

[20] A. S. Lemine, M. M. Zagho, T. M. Altahtamouni and N. Bensalah, "Graphene a promising electrode material for supercapacitors-A review," *International Journal of Energy Research,* vol. 42, no. 14, pp. 4284-4300, 2018.

[21] G. A. Snook, P. Kao and A. S. Best, "Conducting-polymer-based supercapacitor devices and electrodes," *Journal of Power Sources,* vol. 196, no. 1, pp. 1-12, 2011.

[22] D. Saha, Y. Li, Z. Bi, J. Chen, J. K. Keum, D. K. Hensley, H. A. Grappe, H. M. Meyer, S. Dai, M. P. Paranthaman and A. K. Naskar,

"Studies on Supercapacitor Electrode Material from Activated Lignin-Derived Mesoporous Carbon," *Langmuir,* vol. 30, no. 3, pp. 900-910, 2014.

[23] C. Peng, X.-b. Yan, R.-t. Wang, J.-w. Lang, Y.-j. Ou and Q.-j. Xue, "Promising activated carbons derived from waste tea-leaves and their application in high performance supercapacitors electrodes," *Electrochimica Acta,* vol. 87, pp. 401-408, 2013.

[24] M. Zhi, F. Yang, F. Meng, M. Li, A. Manivannan and N. Wu, "Effects of Pore Structure on Performance of An Activated-Carbon Supercapacitor Electrode Recycled from Scrap Waste Tires," *ACS Sustainable Chemistry & Engineering,* vol. 2, no. 7, pp. 1592-1598, 2014.

[25] G. Hegde, S. A. A. Manaf, A. Kumar, G. A. M. Ali, K. F. Chong, Z. Ngaini and K. V. Sharma, "Biowaste Sago Bark Based Catalyst Free Carbon Nanospheres: Waste to Wealth Approach," *ACS Sustainable Chemistry & Engineering,* vol. 3, no. 9, pp. 2247-2253, 2015.

[26] L. L. Zhang and X. S. Zhao, "Carbon-based materials as supercapacitor electrodes," *Chemical Society Reviews,* vol. 38, no. 9, pp. 2520-2531, 2009.

[27] M. Dhelipan, A. Arunchander, A. Sahu and D. Kalpana, "Activated carbon from orange peels as supercapacitor electrode and catalyst support for oxygen reduction reaction in proton exchange membrane fuel cell," *Journal of Saudi Chemical Society,* vol. 21, no. 4, pp. 487-494, 2017.

[28] J. Xu, L. Chen, H. Qu, Y. Jiao, J. Xie and G. Xing, "Preparation and characterization of activated carbon from reedy grass leaves by chemical activation with H3PO4," *Applied Surface Science,* vol. 320, pp. 674-680, 2014.

[29] P. González-García, "Activated carbon from lignocellulosics precursors: A review of the synthesis methods, characterization techniques and applications," *Renewable and Sustainable Energy Reviews,* vol. 82, pp. 1393-1414, 2018.

[30] J. D. L. Fuente, "Graphene Supercapacitors - What Are They?," 2019. [Online]. Available: https://www.graphenea.com/pages/graphene-supercapacitors#.Xdz_B-gzZPY. [Accessed 18 11 2019].

[31] "The Graphene Council," 2019. [Online]. Available: https:// www.thegraphenecouncil.org/default.aspx?page=Supercapcitor. [Accessed 18 11 2019].

[32] L. L. Zhang, R. Zhou and X. S. Zhao, "Graphene-based materials as supercapacitor electrodes," *Journal of Materials Chemistry,* vol. 20, no. 29, p. 5893, 2010.

[33] J. Li, X. Huang, L. Cui, N. Chen and L. Qu, "Preparation and

supercapacitor performance of assembled graphene fiber and foam," *Progress in Natural Science: Materials International,* vol. 26, no. 3, pp. 212-220, 2016.

[34] I. Khakpour, A. R. Baboukani, A. Allagui and C. Wang, "Bipolar Exfoliation and in Situ Deposition of High-Quality Graphene for Supercapacitor Application," *ACS Applied Energy Materials,* vol. 2, no. 7, pp. 4813-4820, 2019.

[35] Z. Fan, Q. Zhao, T. Li, J. Yan, Y. Ren, J. Feng and T. Wei, "Easy synthesis of porous graphene nanosheets and their use in supercapacitors," *Carbon,* vol. 50, no. 4, pp. 1699-1703, 2012.

[36] P. Xu, J. Kang, J.-B. Choi, J. Suhr, J. Yu, F. Li, J.-H. Byun, B.-S. Kim and T.-W. Chou, "Laminated Ultrathin Chemical Vapor Deposition Graphene Films Based Stretchable and Transparent High-Rate Supercapacitor," *ACS Nano,* vol. 8, no. 9, pp. 9437-9445, 2014.

[37] N. A. Kumar and J.-B. Baek, "Doped graphene supercapacitors," *Nanotechnology,* vol. 26, no. 49, p. 492001, 2015.

[38] N. A. Kumar, H. Nolan, N. McEvoy, E. Rezvani, R. L. Doyle, M. E. G. Lyons and G. S. Duesberg, "Plasma-assisted simultaneous reduction and nitrogen doping of graphene oxide nanosheets," *Journal of Materials Chemistry A,* vol. 1, no. 14, p. 4431, 2013.

[39] Z.-Y. Sui, Y.-N. Meng, P.-W. Xiao, Z.-Q. Zhao, Z.-X. Wei and B.-H. Han, "Nitrogen-Doped Graphene Aerogels as Efficient Supercapacitor Electrodes and Gas Adsorbents," *ACS Applied Materials & Interfaces,* vol. 7, no. 3, pp. 1431-1438, 2015.

[40] D. Liu, C. Fu, N. Zhang, H. Zhou and Y. Kuang, "Three-Dimensional Porous Nitrogen doped Graphene Hydrogel for High Energy Density supercapacitors," *Electrochimica Acta,* vol. 213, pp. 291-297, 2016.

[41] H. Peng, G. Ma, K. Sun, Z. Zhang, Q. Yang, F. Ran and Z. Lei, "A facile and rapid preparation of highly crumpled nitrogen-doped graphene-like nanosheets for high-performance supercapacitors," *Journal of Materials Chemistry A,* vol. 3, no. 25, pp. 13210-13214, 2015.

[42] J.-P. Randin and E. Yeager, "Effect of boron addition on the differential capacitance of stress-annealed pyrolytic graphite," *Journal of Electroanalytical Chemistry and Interfacial Electrochemistry,* vol. 54, no. 1, pp. 93-100, 1974.

[43] L. Niu, Z. Li, W. Hong, J. Sun, Z. Wang, L. Ma, J. Wang and S. Yang, "Pyrolytic synthesis of boron-doped graphene and its application as electrode material for supercapacitors," *Electrochimica Acta,* vol. 108, pp. 666-673, 2013.

[44] P. Chen, J.-J. Yang, S.-S. Li, Z. Wang, T.-Y. Xiao, Y.-H. Qian and S.-H. Yu, "Hydrothermal synthesis of macroscopic nitrogen-doped

graphene hydrogels for ultrafast supercapacitor," *Nano Energy,* vol. 2, no. 2, pp. 249-256, 2013.

[45] S.-M. Jung, E. K. Lee, M. Choi, D. Shin, I.-Y. Jeon, J.-M. Seo, H. Y. Jeong, N. Park, J. H. Oh and J.-B. Baek, "Direct Solvothermal Synthesis of B/N-Doped Graphene," *Angewandte Chemie,* vol. 126, no. 9, pp. 2430-2433, 2014.

[46] Z.-S. Wu, A. Winter, L. Chen, Y. Sun, A. Turchanin, X. Feng and K. Müllen, "Three-Dimensional Nitrogen and Boron Co-doped Graphene for High-Performance All-Solid-State Supercapacitors," *Advanced Materials,* vol. 24, no. 37, pp. 5130-5135, 2012.

[47] Z. Chen, L. Hou, Y. Cao, Y. Tang and Y. Li, "Gram-scale production of B, N co-doped graphene-like carbon for high performance supercapacitor electrodes," *Applied Surface Science,* vol. 435, pp. 937-944, 2018.

[48] D. Hulicova-Jurcakova, A. M. Puziy, O. I. Poddubnaya, F. Suárez-García, J. M. D. Tascón and G. Q. Lu, "Highly Stable Performance of Supercapacitors from Phosphorus-Enriched Carbons," *Journal of the American Chemical Society,* vol. 131, no. 14, pp. 5026-5027, 2009.

[49] P. Karthika, N. Rajalakshmi and K. S. Dhathathreyan, "Phosphorus-Doped Exfoliated Graphene for Supercapacitor Electrodes," *Journal of Nanoscience and Nanotechnology,* vol. 13, no. 3, pp. 1746-1751, 2013.

[50] Y. Wen, B. Wang, C. Huang, L. Wang and D. Hulicova-Jurcakova, "Synthesis of Phosphorus-Doped Graphene and its Wide Potential Window in Aqueous Supercapacitors," *Chemistry - A European Journal,* vol. 21, no. 1, pp. 80-85, 2014.

[51] T. Guan, L. Shen and N. Bao, "Hydrophilicity Improvement of Graphene Fibers for High-Performance Flexible Supercapacitor," *Industrial & Engineering Chemistry Research,* vol. 58, no. 37, pp. 17338-17345, 2019.

[52] S. Wang, N. Liu, J. Su, L. Li, F. Long, Z. Zou, X. Jiang and Y. Gao, "Highly Stretchable and Self-Healable Supercapacitor with Reduced Graphene Oxide Based Fiber Springs," *ACS Nano,* vol. 11, no. 2, pp. 2066-2074, 2017.

[53] S. Chen, W. Ma, Y. Cheng, Z. Weng, B. Sun, L. Wang, W. Chen, F. Li, M. Zhu and H.-M. Cheng, "Scalable non-liquid-crystal spinning of locally aligned graphene fibers for high-performance wearable supercapacitors," *Nano Energy,* vol. 15, pp. 642-653, 2015.

[54] G. Qu, J. Cheng, X. Li, D. Yuan, P. Chen, X. Chen, B. Wang and H. Peng, "A Fiber Supercapacitor with High Energy Density Based on Hollow Graphene/Conducting Polymer Fiber Electrode," *Advanced Materials,* vol. 28, no. 19, pp. 3646-3652, 2016.

[55] Z. Yang, J. Deng, X. Chen, J. Ren and H. Peng, "A Highly Stretchable,

Fiber-Shaped Supercapacitor," *Angewandte Chemie International Edition,* vol. 52, no. 50, pp. 13453-13457, 2013.

[56] X. Li, T. Zhao, K. Wang, Y. Yang, J. Wei, F. Kang, D. Wu and H. Zhu, "Directly Drawing Self-Assembled, Porous, and Monolithic Graphene Fiber from Chemical Vapor Deposition Grown Graphene Film and Its Electrochemical Properties," *Langmuir,* vol. 27, no. 19, pp. 12164-12171, 2011.

[57] G. Huang, C. Hou, Y. Shao, B. Zhu, B. Jia, H. Wang, Q. Zhang and Y. Li, "High-performance all-solid-state yarn supercapacitors based on porous graphene ribbons," *Nano Energy,* vol. 12, pp. 26-32, 2015.

[58] H. H. Shi, S. Jang and H. E. Naguib, "Freestanding Laser-Assisted Reduced Graphene Oxide Microribbon Textile Electrode Fabricated on a Liquid Surface for Supercapacitors and Breath Sensors," *ACS Applied Materials & Interfaces,* vol. 11, no. 30, pp. 27183-27191, 2019.

[59] S. Grover, S. Goel, V. Sahu, G. Singh and R. K. Sharma, "Asymmetric Supercapacitive Characteristics of PANI Embedded Holey Graphene Nanoribbons," *ACS Sustainable Chemistry & Engineering,* vol. 3, no. 7, pp. 1460-1469, 2015.

[60] V. Sahu, S. Shekhar, R. K. Sharma and G. Singh, "Ultrahigh Performance Supercapacitor from Lacey Reduced Graphene Oxide Nanoribbons," *ACS Applied Materials & Interfaces,* vol. 7, no. 5, pp. 3110-3116, 2015.

[61] M. Khandelwal and A. Kumar, "One-step chemically controlled wet synthesis of graphene nanoribbons from graphene oxide for high performance supercapacitor applications," *Journal of Materials Chemistry A,* vol. 3, no. 45, pp. 22975-22988, 2015.

[62] T. Kuilla, S. Bhadra, D. Yao, N. H. Kim, S. Bose and J. H. Lee, "Recent advances in graphene based polymer composites," *Progress in Polymer Science,* vol. 35, no. 11, pp. 1350-1375, 2010.

[63] C. Xiang, Y. Liu, Y. Yin, P. Huang, Y. Zou, M. Fehse, Z. She, F. Xu, D. Banerjee, D. H. Merino, A. Longo, H.-B. Kraatz, D. F. Brougham, B. Wu and L. Sun, "Facile Green Route to Ni/Co Oxide Nanoparticle Embedded 3D Graphitic Carbon Nanosheets for High Performance Hybrid Supercapacitor Devices," *ACS Applied Energy Materials,* vol. 2, no. 5, pp. 3389-3399, 2019.

[64] J. Chen, Y. Wang, J. Cao, Y. Liu, Y. Zhou, J.-H. Ouyang and D. Jia, "Facile Co-Electrodeposition Method for High-Performance Supercapacitor Based on Reduced Graphene Oxide/Polypyrrole Composite Film," *ACS Applied Materials & Interfaces,* vol. 9, no. 23, pp. 19831-19842, 2017.

[65] S. Dhibar, P. Bhattacharya, D. Ghosh, G. Hatui and C. K. Das, "Graphene–Single-Walled Carbon Nanotubes–Poly(3-

methylthiophene) Ternary Nanocomposite for Supercapacitor Electrode Materials," *Industrial & Engineering Chemistry Research,* vol. 53, no. 33, pp. 13030-13045, 2014.

[66] G. Zhang, Y. Chen, Y. Deng and C. Wang, "A Triblock Copolymer Design Leads to Robust Hybrid Hydrogels for High-Performance Flexible Supercapacitors," *ACS Applied Materials & Interfaces,* vol. 9, no. 41, pp. 36301-36310, 2017.

[67] L.-l. Jiang, X. Lu, C.-m. Xie, G.-j. Wan, H.-p. Zhang and T. Youhong, "Flexible, Free-Standing TiO2–Graphene–Polypyrrole Composite Films as Electrodes for Supercapacitors," *The Journal of Physical Chemistry C,* vol. 119, no. 8, pp. 3903-3910, 2015.

[68] L. Halder, A. Maitra, A. K. Das, R. Bera, S. K. Karan, S. Paria, A. Bera, S. K. Si and B. B. Khatua, "Fabrication of an Advanced Asymmetric Supercapacitor Based on Three-Dimensional Copper–Nickel–Cerium–Cobalt Quaternary Oxide and GNP for Energy Storage Application," *ACS Applied Electronic Materials,* vol. 1, no. 2, pp. 189-197, 2019.

[69] R. Kumar, R. K. Singh, P. K. Dubey, D. P. Singh and R. M. Yadav, "Self-Assembled Hierarchical Formation of Conjugated 3D Cobalt Oxide Nanobead–CNT–Graphene Nanostructure Using Microwaves for High-Performance Supercapacitor Electrode," *ACS Applied Materials & Interfaces,* vol. 7, no. 27, pp. 15042-15051, 2015.

[70] C. Zhang, B. Zheng, C. Huang, Y. Li, J. Wang, S. Tang, M. Deng and Y. Du, "Heterostructural Three-Dimensional Reduced Graphene Oxide/CoMn2O4 Nanosheets toward a Wide-Potential Window for High-Performance Supercapacitors," *ACS Applied Energy Materials,* vol. 2, no. 7, pp. 5219-5230, 2019.

[71] Y. Cheng, Y. Zhang and C. Meng, "Template Fabrication of Amorphous Co2SiO4 Nanobelts/Graphene Oxide Composites with Enhanced Electrochemical Performances for Hybrid Supercapacitors," *ACS Applied Energy Materials,* vol. 2, no. 5, pp. 3830-3839, 2019.

[72] S. Wu, C. Liu, D. A. Dinh, K. S. Hui, K. N. Hui, J. M. Yun and K. H. Kim, "Three-Dimensional Self-Standing and Conductive MnCO3@Graphene/CNT Networks for Flexible Asymmetric Supercapacitors," *ACS Sustainable Chemistry & Engineering,* vol. 7, no. 11, pp. 9763-9770, 2019.

[73] H. Jiang, X. Ye, Y. Zhu, Z. Yue, L. Wang, J. Xie, Z. Wan and C. Jia, "Flexible Solid-State Supercapacitors with High Areal Performance Enabled by Chlorine-Doped Graphene Films with Commercial-Level Mass Loading," *ACS Sustainable Chemistry & Engineering,* 2019.

[74] Z. Xu, Z. Li, C. M. B. Holt, X. Tan, H. Wang, B. S. Amirkhiz, T.

Stephenson and D. Mitlin, "Electrochemical Supercapacitor Electrodes from Sponge-like Graphene Nanoarchitectures with Ultrahigh Power Density," *The Journal of Physical Chemistry Letters,* vol. 3, no. 20, pp. 2928-2933, 2012.

[75] H.-C. Chen, Y.-C. Lin, Y.-L. Chen and C.-J. Chen, "Facile Fabrication of Three-Dimensional Hierarchical Nanoarchitectures of VO2/Graphene@NiS2 Hybrid Aerogel for High-Performance All-Solid-State Asymmetric Supercapacitors with Ultrahigh Energy Density," *ACS Applied Energy Materials,* vol. 2, no. 1, pp. 459-467, 2018.

[76] C. Liu, X. Zhao, S. Wang, Y. Zhang, W. Ge, J. Li, J. Cao, J. Tao and X. Yang, "Freestanding, Three-Dimensional, and Conductive MoS2 Hydrogel via the Mediation of Surface Charges for High-Rate Supercapacitor," *ACS Applied Energy Materials,* vol. 2, no. 6, pp. 4458-4463, 2019.

[77] N. A. Elessawy, J. E. Nady, W. Wazeer and A. B. Kashyout, "Development of High-Performance Supercapacitor based on a Novel Controllable Green Synthesis for 3D Nitrogen Doped Graphene," *Scientific Reports,* vol. 9, no. 1, 2019.

[78] H. Wan, J. Liu, Y. Ruan, L. Lv, L. Peng, X. Ji, L. Miao and J. Jiang, "Hierarchical Configuration of NiCo2S4 Nanotube@Ni–Mn Layered Double Hydroxide Arrays/Three-Dimensional Graphene Sponge as Electrode Materials for High-Capacitance Supercapacitors," *ACS Applied Materials & Interfaces,* vol. 7, no. 29, pp. 15840-15847, 2015.

[79] Y. Li, S. Liu, Y. Liang, Y. Xiao, H. Dong, M. Zheng, H. Hu and Y. Liu, "Bark-Based 3D Porous Carbon Nanosheet with Ultrahigh Surface Area for High Performance Supercapacitor Electrode Material," *ACS Sustainable Chemistry & Engineering,* vol. 7, no. 16, pp. 13827-13835, 2019.

[80] S. R. Mangisetti, M. Kamaraj and R. Sundara, "Green Approach for Synthesizing Three Different Carbon Microstructures from a Single Biowaste Bombax malabaricum for Fully Biocompatible Flexible Supercapacitors and Their Performance in Various Electrolytes," *ACS Omega,* vol. 4, no. 4, pp. 6399-6410, 2019.

[81] T. Chen, J. Zhang, P. Shi, Y. Li, L. Zhang, Z. Sun, R. He, T. Duan and W. Zhu, "Thalia dealbata Inspired Anisotropic Cellular Biomass Derived Carbonaceous Aerogel," *ACS Sustainable Chemistry & Engineering,* vol. 6, no. 12, pp. 17152-17159, 2018.

[82] F. Hekmat, S. Shahrokhian and N. Taghavinia, "Ultralight Flexible Asymmetric Supercapacitors Based On Manganese Dioxide–Polyaniline Nanocomposite and Reduced Graphene Oxide Electrodes Directly Deposited on Foldable Cellulose Papers," *The*

Journal of Physical Chemistry C, vol. 122, no. 48, pp. 27156-27168, 2018.

[83] K. Nanaji, V. Upadhyayula, T. N. Rao and S. Anandan, "Robust, Environmentally Benign Synthesis of Nanoporous Graphene Sheets from Biowaste for Ultrafast Supercapacitor Application," *ACS Sustainable Chemistry & Engineering,* vol. 7, no. 2, pp. 2516-2529, 2018.

[84] F. Gao, J. Qu, Z. Zhao, Z. Wang and J. Qiu, "Nitrogen-doped activated carbon derived from prawn shells for high-performance supercapacitors," *Electrochimica Acta,* vol. 190, pp. 1134-1141, 2016.

[85] Y. Jiao, C. Qu, B. Zhao, Z. Liang, H. Chang, S. Kumar, R. Zou, M. Liu and K. S. Walton, "High-Performance Electrodes for a Hybrid Supercapacitor Derived from a Metal–Organic Framework/Graphene Composite," *ACS Applied Energy Materials,* vol. 2, no. 7, pp. 5029-5038, 2019.

[86] M. Chandel, P. Makkar and N. N. Ghosh, "Ag–Ni Nanoparticle Anchored Reduced Graphene Oxide Nanocomposite as Advanced Electrode Material for Supercapacitor Application," *ACS Applied Electronic Materials,* vol. 1, no. 7, pp. 1215-1224, 2019.

[87] S. Sundriyal, V. Shrivastav, H. Kaur, S. Mishra and A. Deep, "High-Performance Symmetrical Supercapacitor with a Combination of a ZIF-67/rGO Composite Electrode and a Redox Additive Electrolyte," *ACS Omega,* vol. 3, no. 12, pp. 17348-17358, 2018.

[88] W. Zhang, B. Quan, C. Lee, S.-K. Park, X. Li, E. Choi, G. Diao and Y. Piao, "One-Step Facile Solvothermal Synthesis of Copper Ferrite–Graphene Composite as a High-Performance Supercapacitor Material," *ACS Applied Materials & Interfaces,* vol. 7, no. 4, pp. 2404-2414, 2015.

[89] Q. Chang, L. Li, H. Qiao, L. Sai, Y. Zhang, W. Shi and L. Huang, "Enhanced Electrolyte Ion Penetration in Microdome-like Graphene with High Mass Loading for High-Performance Flexible Supercapacitors," *ACS Applied Energy Materials,* vol. 2, no. 9, pp. 6790-6799, 2019.

[90] S. Wang, J. Shen, Q. Wang, Y. Fan, L. Li, K. Zhang, L. Yang, W. Zhang and X. Wang, "High-Performance Layer-by-Layer Self-Assembly PANI/GQD-rGO/CFC Electrodes for a Flexible Solid-State Supercapacitor by a Facile Spraying Technique," *ACS Applied Energy Materials,* vol. 2, no. 2, pp. 1077-1085, 2019.

[91] H. H. Hsu, A. Khosrozadeh, B. Li, G. Luo, M. Xing and W. Zhong, "An Eco-Friendly, Nanocellulose/RGO/in Situ Formed Polyaniline for Flexible and Free-Standing Supercapacitors," *ACS Sustainable Chemistry & Engineering,* vol. 7, no. 5, pp. 4766-4776, 2019.

[92] Y. Wu, J. Zhu and L. Huang, "A review of three-dimensional graphene-based materials: Synthesis and applications to energy

conversion/storage and environment," *Carbon,* vol. 143, pp. 610-640, 2019.

[93] B. Jia, "Graphene supercapcitors for electric vehicles".

[94] L. Manjakkal, C. G. Núñez, W. Dang and R. Dahiya, "Flexible Self-Charging Supercapacitor Based on Graphene-Ag-3D Graphene Foam Electrodes," *Nano Energy,* no. 51, pp. 604-612, 2018.

[95] B. K. Kim, S. Sy, A. Yu and J. Zhang, "Electrochemical Supercapacitors for Energy Storage and Conversion," *Handbook of Clean Energy Systems,* pp. 1-25, 2015.

[96] electrive.com, "Solaris delivers eleven hybrid buses to Romania," 19 11 2019. [Online]. Available: https:// www.electrive.com/ 2019/ 11/ 19/solaris-delivers-eleven-hybrid-buses-to-romania/. [Accessed 23 11 2019].

[97] W. Contributors, "Wikipedia," 25 9 2019. [Online]. Available: https://en.wikipedia.org/wiki/Capa_vehicle. [Accessed 23 11 2019].

[98] P. Patel, "A Battery-Ultracapacitor Hybrid," 2019. [Online]. Available: https://www.technologyreview.com/s/417053/a-battery- ultracapacitor-hybrid/.

[99] C. K. Emre O. Polat, "Broadband Optical Modulators Based on Graphene Supercapacitors," *Nano Letters,* vol. 13, no. 12, pp. 5851-5857, 2013.

[100] "Biosolar.com," 2019. [Online]. Available: <http:// www.biosolar.com/ biosupercap.php>.

[101] Tecate Group, "Tecate Group - Markets & Applications.," 2019. [Online]. Available: https:// www.tecategroup.com/ markets/ ? market=Military-Aerospace. [Accessed 23 11 2019].

[102] B. Xie, C. Yang, Z. Zhang, P. Zou, Z. Lin, G. Shi, Q. Yang, F. Kang and C.-P. Wong, "Shape-Tailorable Graphene-Based Ultra-High-Rate Supercapacitor for Wearable Electronics," *ACS Nano,* vol. 9, no. 6, pp. 5636-5645, 2015.

[103] L. Francioso, C. D. Pascali, I. Farella, C. Martucci, P. Cretì, P. Siciliano and A. Perrone, "Flexible thermoelectric generator for ambient assisted living wearable biometric sensors," *Journal of Power Sources,* vol. 196, no. 6, p. 3239–3243, 2011.

[104] A. Yu, I. Roes, A. Davies and Z. Chen, "Ultrathin, transparent and flexible graphene films for supercapacitor applications," *Applied Physics Letters,* vol. 96, no. 25, p. 253105, 2010.

[105] H. Shuijian and C. Wei, "Application of biomass-derived flexible carbon cloth coated with MnO2 nanosheets in supercapacitors," *Journal of Power Sources,* vol. 294, pp. 150-158, 2015.

[106] L. V. Thekkekara and M. Gu, "Large-scale waterproof and stretchable textile-integrated laser- printed graphene energy storages," *Scientific reports,* vol. 9, no. 1, 2019.